THE JOURNAL OF BIOLOGICAL CHEMISTRY VOL. 284, NO. 11, pp. 6841–6849, March 13, 2009

Heat-shock Protein 90 Is Essential for Stabilization of the Hepatitis C Virus Nonstructural Protein NS3*

Received for publication, August 20, 2008, and in revised form, December 22, 2008 Published, JBC Papers in Press, January 16, 2009, DOI 10.1074/jbc.M806452200

Saneyuki Ujino[‡], **Saori Yamaguchi**[‡], **Kunitada Shimotohno**[§¶], **and Hiroshi Takaku**[‡‖1]

From the [‡]*Department of Life and Environmental Sciences,* [‖]*High Technology Research Center, and* [§]*Research Institute, Chiba Institute of Technology, 2-17-1 Tsudanuma, Narashino, Chiba 275-0016, Japan and the* [¶]*Center for Integrated Medical Research, School of Medicine, Keio University, Shinanomachi, Tokyo 160-8582, Japan*

The hepatitis C virus (HCV) is a major cause of chronic liver disease. Here, we report a new and effective strategy for inhibiting HCV replication using 17-allylaminogeldanamycin (17-AAG), an inhibitor of heat-shock protein 90 (Hsp90). Hsp90 is a molecular chaperone with a key role in stabilizing the conformation of many oncogenic signaling proteins. We examined the inhibitory effects of 17-AAG on HCV replication in an HCV replicon cell culture system. In HCV replicon cells treated with 17-AAG, we found that HCV RNA replication was suppressed in a dose-dependent manner, and interestingly, the only HCV protein degraded in these cells was NS3 (nonstructural protein 3). Immunoprecipitation experiments showed that NS3 directly interacted with Hsp90, as did proteins expressed from ΔNS3 protease expression vectors. These results suggest that the suppression of HCV RNA replication is due to the destabilization of NS3 in disruption of the Hsp90 chaperone complex by 17-AAG.

Infection by the hepatitis C virus (HCV)[2] is a major public health problem, with 170 million chronically infected people worldwide (1, 2). The current treatment by combined interferon-ribavirin therapy fails to cure the infection in 30–50% of cases (3, 4), particularly those with HCV genotypes 1 and 2. Chronic infection with HCV results in liver cirrhosis and can lead to hepatocellular carcinoma (5, 6). Although an effective combined interferon-α-ribavirin therapy is available for about 50% of the patients with HCV, better therapies are needed, and preventative vaccines have not yet been developed.

HCV is a member of the *Flaviviridae* family and has a positive strand RNA genome (7, 8) that encodes a large precursor polyprotein, which is cleaved by host and viral proteases to generate at least 10 functional viral proteins: core, E1 (envelope 1), E2, p7, NS2 (nonstructural protein 2), NS3, NS4A, NS4B, NS5A, and NS5B (9, 10). NS2 and the amino terminus of NS3 comprise the NS2-3 protease responsible for cleavage between NS2 and NS3 (9, 11), whereas NS3 is a multifunctional protein consisting of an amino-terminal protease domain required for processing NS3 to NS5B (12, 13). NS4A is a cofactor that activates the NS3 protease function by forming a heterodimer (14–17), and the hydrophobic protein NS4B induces the formation of a cytoplasmic vesicular structure, designated the membranous web, which is likely to contain the replication complex of HCV (18, 19). NS5A is a phosphoprotein that appears to play an important role in viral replication (20–23), and NS5B is the RNA-dependent RNA polymerase of HCV (24, 25). The 3′-untranslated region consists of a short variable sequence, a poly(U)-poly(UC) tract, and a highly conserved X region and is critical for HCV RNA replication and HCV infection (26–29).

Hsp90 (heat-shock protein 90) is a molecular chaperone that plays a key role in the conformational maturation of many cellular proteins. Hsp90 normally functions in association with other co-chaperone proteins, which together play an important role in folding newly synthesized proteins and stabilizing and refolding denatured proteins in cells subjected to stress (30–34). Its expression is induced by cellular stress and is also associated with many types of tumor. Hsp90 inhibitors are currently showing great promise as novel pharmacological agents for anticancer therapy.

Hsp90 inhibitors have two major modes of action as preferential clients for protein degradation or as Hsp70 inducers. The benzoquinone ansamycin antibiotic geldanamycin and its less toxic analogue 17-allylamino-17-demethoxygeldanamycin (17-AAG) directly bind to the ATP/ADP binding pocket of Hsp90 (34–36) and thus prevent ATP binding and the completion of client protein refolding. Recently, Waxman *et al.* (37) demonstrated a role for Hsp90 in promoting the cleavage of HCV NS2/3 protease, using NS2/3 translated by rabbit reticulocyte lysate. Nakagawa *et al.* (38) also reported that inhibition of Hsp90 is highly effective in suppressing HCV genome replication. Hsp90 may directly or indirectly interact with any of the proteins NS3 through NS5B to regulate replication of the HCV replicon. More recently, Okamoto *et al.* (39) reported that Hsp90 could bind to FKBP8 (FK506-binding protein 8) and form a complex with NS5A. The interaction with FKBP8 has also been shown to be the mechanism by which Hsp90 regulates HCV RNA replication, a process in which Hsp90 clearly plays an important role.

In this study, we have demonstrated that NS3 also forms a complex with Hsp90, which is critical for HCV replication. On the basis of the findings that treating HCV replicon cells with

* This work was supported by a grant-in-aid for HCV research from the Ministry of Health, Labor, and Welfare of Japan and by a grant-in-aid for high technology research from the Ministry of Education, Science, Sports, and Culture of Japan. The costs of publication of this article were defrayed in part by the payment of page charges. This article must therefore be hereby marked "*advertisement*" in accordance with 18 U.S.C. Section 1734 solely to indicate this fact.

[1] To whom correspondence should be addressed: Dept. of Life and Environmental Science and High Technology Research Center, Chiba Institute of Technology, 2-17-1 Tsudanuma, Narashino-shi, Chiba 275-0016, Japan. Tel.: 81-47-478-0407; Fax: 81-47-471-8764; E-mail: hiroshi.takaku@it-chiba.ac.jp.

[2] The abbreviations used are: HCV, hepatitis C virus; 17-AAG, 17-allylamino-17-demethoxygeldanamycin.

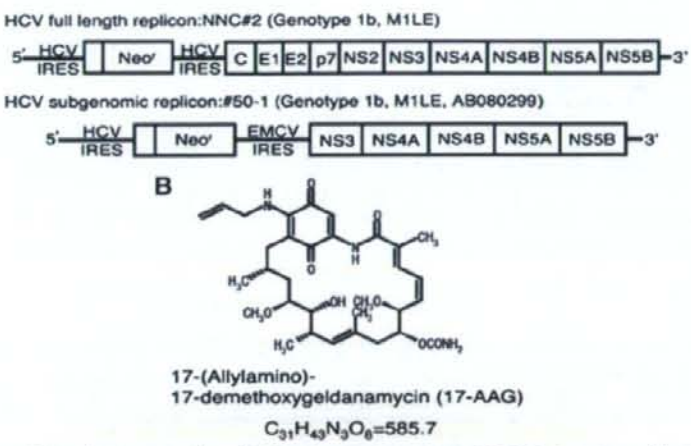

FIGURE 1. **Schematic representation of HCV replicon and structure of 17-AAG.** *A*, structure of the HCV replicon RNAs, comprising the HCV 5′-untranslated region, including the HCV internal ribosome entry site (*IRES*), the neomycin phosphotransferase gene (*Neo'*), the encephalomyocarditis virus (*EMCV*) IRES or HCV IRES, and the coding region for HCV proteins NS3 to NS5B (in the HCV subgenomic replicon) or core to NS5B (in the HCV full-length replicon). *B*, structures of the Hsp90 inhibitor, 17-AAG.

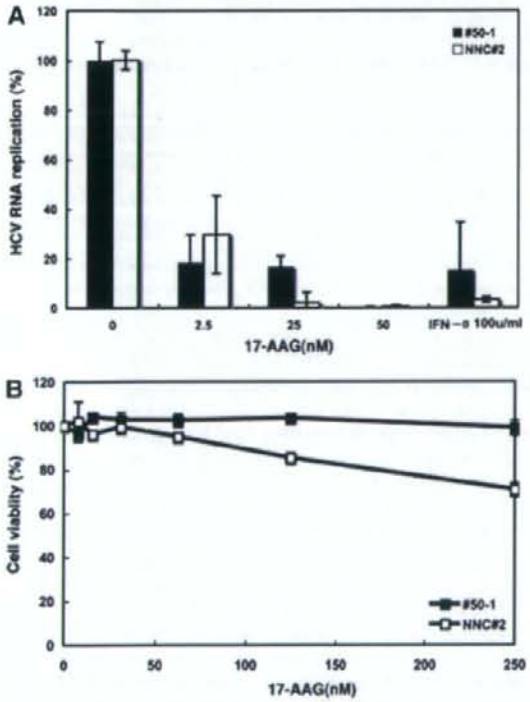

FIGURE 2. **Hsp90 inhibits HCV RNA replication in HCV replicon cells.** *A*, inhibition of HCV replication by 17-AAG in NNC#2 (*white squares*) and #50-1 cells (*black squares*) measured by real time reverse transcription-PCR after 72 h. Interferon-α was used as a positive control. The data are means ± S.D. from triplicate experiments. *B*, cytotoxic effects of 17-AAG in NNC#2 (*white squares*) and #50-1 (*black squares*), shown as the percentage reduction in viable cell numbers in an [3-(4,5-dimethylthiazol-2-yl)-5-(3-carboxymethoxyphenyl)-2-(4-sulfophenyl)-2H-tetrazolium (inner salt)] assay. The data are means ± S.D. from triplicate experiments.

the Hsp90 inhibitor, 17-AAG, suppressed HCV RNA replication, and that the only HCV protein degraded in these cells was NS3, we suggest a crucial role for Hsp90-NS3 protein complexes in the HCV life cycle.

EXPERIMENTAL PROCEDURES

Cell Culture and Reagents—The HCV replicon cell lines #50-1 (NN/1b/SG) (40), which carries a subgenomic replicon, and NNC#2 (NN/1b/FL) (41), which carries a full genome replicon, were cultured in Dulbecco's modified Eagle's medium supplemented with 10% fetal bovine serum, nonessential amino acids, L-glutamine, penicillin/streptomycin, and 300–1,000 μg/ml G418 (Invitrogen) at 37 °C in 5% CO_2. The human embryonic kidney-derived cell line 293T was grown in Dulbecco's modified Eagle's medium supplemented with 10% fetal bovine serum, 100 units/ml penicillin, and 100 μg/ml streptomycin. 17-AAG was purchased from Sigma.

Measuring HCV RNA by Real Time PCR—HCV replicon cells were seeded at 1.5×10^5 cells in 24-well plates and cultured for 72 h. Total RNA was then isolated using TRIzol (Invitrogen) according to the manufacturer's instructions. HCV RNA was quantified by real time reverse transcription-PCR using an ABI 7700 sequence detector (PerkinElmer Life Sciences) and the following primers and TaqMan probes located in the 5′-untranslated region: forward primer (nucleotides 130–146), 5′-CGGGAGAGCCATAGTGG-3′; reverse primer (nucleotides 272–290), 5′-AGTACCACAAGGCCTTTCG-3′; and TaqMan probe (nucleotides 148–168), 5′-CTGCGGAACCG-GTGAGTACAC-3′ (all purchased from Applied Biosystems). The probe sequence was labeled with the reporter dye, 6-carboxyflurorescein, at the 5′-end and with the quencher dye TAMRA at the 3′-end (42).

Western Blotting and Immunoprecipitation Analyses—Cells were lysed in 1× CAT enzyme-linked immunosorbent assay buffer (Roche Applied Sciences). Cell lysates were separated by SDS-PAGE and transferred to nitrocellulose membranes, and these were blocked with 5% skimmed milk. The primary antibodies used were monoclonal or polyclonal antibody against FLAG-M5 (Sigma), Hsp70 (Sigma), Hsp90 (Cell Signaling Technologies, Danvers, MA), Hsp90α (Calbiochem), Hsp90β (Calbiochem), and Hsf-1 (Calbiochem). Core, NS4A, and NS4B were a gift from Dr. M. Kohara (Tokyo Metropolitan Institute of Medical Science). E1, E2, NS3, NS5A, and NS5B were a gift from Prof. Y. Matsuura (Osaka University, Japan). Immunoprecipitation from cell lysates was carried out using anti-FLAG M5 antibody (Sigma) and the Protein G immunoprecipitation kit (Sigma), according to the manufacturer's instructions, and the immunoprecipitates were analyzed by Western blotting.

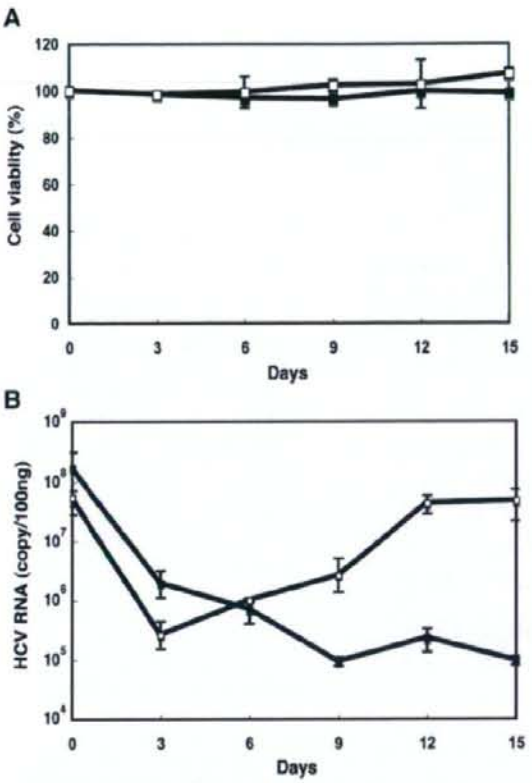

FIGURE 3. **Long term inhibition of HCV replication in NNC#2 cells.** *A*, cytotoxic effect of 17-AAG in NNC#2 cells, shown as the percentage reduction of viable cell numbers assessed by trypan blue staining. NNC#2 cells were treated with 50 nM 17-AAG on day 0 only (*white squares*) or at 3-day intervals for 15 days (*black squares*). The data are means ± S.D. from triplicate experiments. *B*, measurement of HCV replication by real time reverse transcription-PCR. Inhibition of HCV RNA replication in NNC#2 cells treated with 50 nM 17-AAG on day 0 only (*white squares*) or at 3-day intervals for 15 days (*black squares*). *Day 0*, mock. The data are means ± S.D. from triplicate experiments.

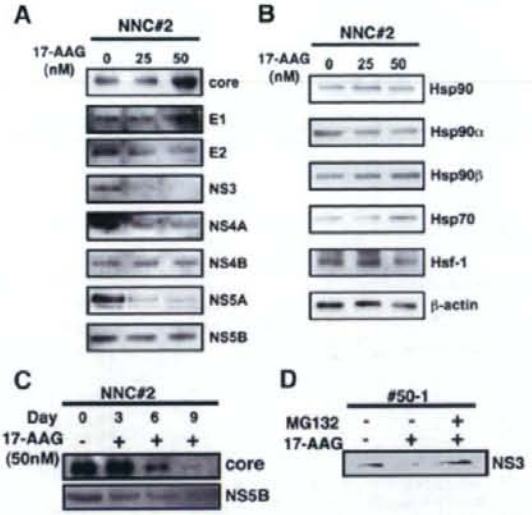

FIGURE 4. **Effect of 17-AAG on HCV NS3 protein levels.** *A*, Western blot analysis of HCV protein expression in NNC#2 or #50-1 cells treated with 17-AAG. NNC#2 or #50-1 cells were treated with 25 and 50 nM 17-AAG for 3 days. Cell lysates were separated by SDS-PAGE, immunoblotted, and probed with antibodies specific for HCV core, E1, E2, NS3, NS4A, NS4B, NS5A, and NS5B. *B*, Western blot analysis of Hsp90, Hsp70, and other chaperone expression in NNC#2 cells treated with 17-AAG (25 and 50 nM, as indicated) for 3 days. *C*, expression of HCV core and NS5B protein in cells treated with 50 nM 17-AAG for 9 days. *D*, effect of 50 nM 17-AAG on NS3 expression in #50-1 cells simultaneously treated with 100 nM MG132.

[3-(4,5-dimethylthiazol-2-yl)-5-(3-carboxymethoxyphenyl)-2-(4-sulfophenyl)-2H-tetrazolium, inner salt Assay—HCV replicon cells were seeded in 96-well plates at 3×10^4 cells/well in a final culture volume of 100 μl for 72 h before the addition of increasing concentrations of 17-AAG. After incubation for 3 days, viable cell numbers were determined using the Celltiter 96 Aqueous nonradioactive cell proliferation assay (Promega Corp., Madison, WI). The value of the background absorbance at 490 nm (A_{490}) of wells without cells was subtracted. The percentages of viable cells were then calculated using the formula, (A_{490} of 17-AAG-treated sample/A_{490} of untreated cells) × 100.

Plasmids and Transfection—The pFLAG-CMV-NS3 vector was constructed by subcloning a DNA fragment encoding full-length NS3, Δhelicase, Δprotease, ΔPH 1, ΔPH 2, and ΔH 1 into the EcoRI and XbaI sites of the pFLAG-CMV™-2 expression vector (Sigma), so that the amino-terminal FLAG epitope was fused in frame with NS3. The core expression vector was a gift from Dr. M. Kohara. The vector was transfected into 293T cells using the FuGENE 6 transfection reagent (Roche Applied Science) according to the manufacturer's instructions.

RESULTS

Hsp90 Inhibitor 17-AAG Suppresses HCV RNA Replication—To investigate the effect of 17-AAG on HCV replication, cells containing a full HCV genome replicon (NNC#2) or a subgenomic replicon (#50-1) were treated with 17-AAG (Fig. 1, *A* and *B*). Both of the HCV replicon cell lines were treated for 72 h with different concentrations of 17-AAG or with DMSO as a control. In cells treated with 50 nM 17-AAG, HCV RNA replication was suppressed by 99% in both of the HCV replicon cell lines, and the inhibition of RNA replication occurred in a dose-dependent manner (Fig. 2*A*). The half-maximal inhibitory concentration (IC_{50}) values of 17-AAG for HCV replication were 0.3 nM in NNC#2 cells and 0.1 nM in #50-1 cells. Furthermore, we used a tetrazolium-based [3-(4,5-dimethylthiazol-2-yl)-5-(3-carboxymethoxyphenyl)-2-(4-sulfophenyl)-2H-tetrazolium, inner salt assay to determine the viability of NNC#2 and #50-1 cells in the presence of 17-AAG. 17-AAG showed no toxicity to NNC#2 and #50-1 cells at 50 nM, (Fig. 2*B*). These results suggested that 17-AAG had a greater inhibitory effect on HCV RNA replication than 100 units/ml interferon-α.

Long Term Suppression of HCV RNA Replication—We next examined the effect of 17-AAG on HCV replication over time. When NNC#2 cells were cultured with 50 nM 17-AAG only on day 0 (*white squares*), the level of HCV RNA was reduced by 2 log on day 3 but had increased to control levels by day 12 (Fig.

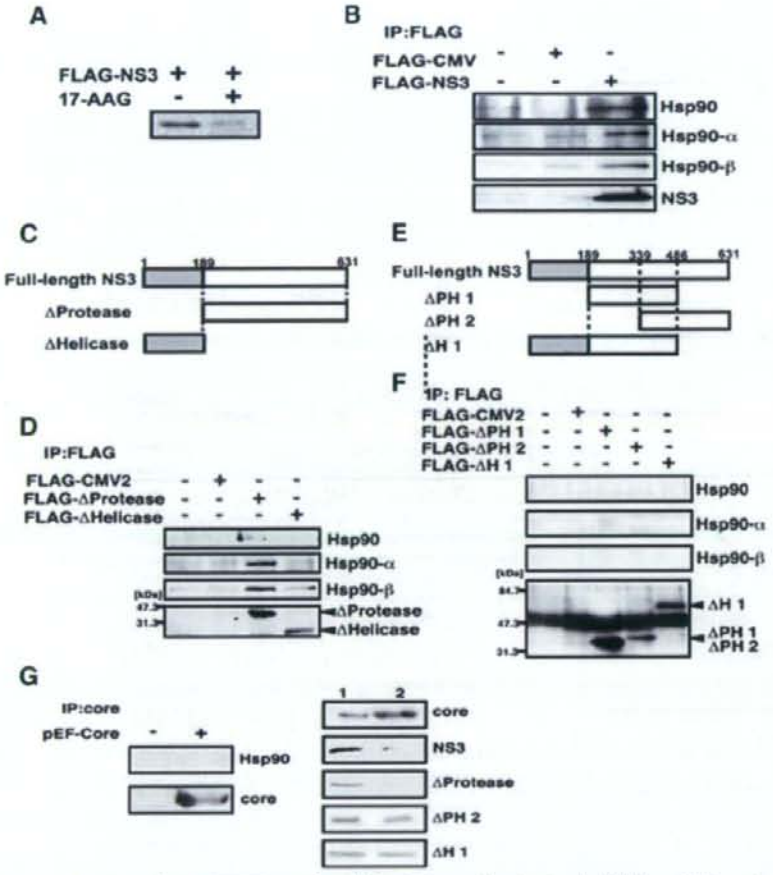

FIGURE 5. **Hsp90 regulates HCV NS3 protein stability.** *A*, Western blot showing the inhibition of NS3 protein expression in 293T cells caused by 17-AAG. Cells were transfected with pFLAG-NS3 in the presence of 250 nM 17-AAG for 48 h. *B*, FLAG-NS3 was expressed in 293T cells and immunoprecipitated (*IP*) from cell lysates with anti-FLAG antibody. Proteins immunoprecipitated were analyzed by Western blotting using anti-Hsp90, anti-Hsp90α, anti-Hsp90β, and anti-FLAG antibodies. The data shown in each *panel* are representative of three independent experiments. *FLAG-CMV*, empty plasmid vector. *C*, schematic representations of HCV NS3 protein and its deletion mutants. *D*, FLAG-NS3, FLAG-Δprotease, and FLAG-Δhelicase were expressed in 293T cells and immunoprecipitated from cell lysates with anti-FLAG antibody. Proteins immunoprecipitated with anti-Hsp90, Hsp90α, Hsp90β, and FLAG antibodies were analyzed by Western blotting. The data shown in each panel are representative of three independent experiments. *E*, schematic representations of HCV NS3 protein and further deletion mutants. *F*, FLAG-ΔPH 1, FLAG-ΔPH 2, and FLAG-ΔH 1 were expressed in 293T cells and immunoprecipitated from cell lysates with anti-FLAG antibody. Proteins immunoprecipitated with anti-Hsp90, Hsp90α, Hsp90β, and FLAG antibodies were analyzed by Western blotting. The data shown in each panel are representative of three independent experiments. *G*, FLAG-NS3, pEF-Core, FLAG-Δprotease, FLAG-ΔPH 2, and FLAG-ΔH 1 were expressed in 293T cells treated with 17-AAG. Proteins immunoprecipitated with anti-core, Hsp90 antibody were analyzed by Western blotting. 17-AAG-treated cell lysates were analyzed on Western blots, using the specific antibodies shown to the *right* of the panels. *Lane 1*, control; *lane 2*, 17-AAG (1 μM).

3*B*). However, when 50 nM 17-AAG was added to the cells at 3-day intervals for 15 days (*black squares*), the observed significant reduction in HCV RNA (by 3 log) was sustained from day 3 to day 15. We used trypan blue staining to check that long term treatment with 17-AAG did not induce cellular toxicity (Fig. 3*A*). Our results suggested that 17-AAG has the potential to safely induce long term suppression in HCV replication.

Reduced Expression of NS3 Protein in 17-AAG-treated HCV Replicon Cells—To investigate the mechanism by which 17-AAG inhibited HCV replication, we analyzed the expression of HCV core, E1, E2, NS3, NS4A, NS4B, NS5A, and NS5B proteins by Western blotting. NNC#2 cells treated with increasing doses of 17-AAG showed a marked reduction in the expression of NS3 (Fig. 4*A*) after 3 days, in common with the level of HCV RNA (Fig. 2*A*). However, levels of the other proteins were unchanged. This dose-dependent inhibition suggested that NS3 was more sensitive to 17-AAG than the other proteins. Similar effects on NS3 expression and RNA replication were seen in #50-1 cells treated with 17-AAG (Fig. 4*A*).

Another effect of 17-AAG treatment seen in these cells was an increase in Hsp70 expression and a slight increase in Hsp90 expression (Fig. 4*B*). The induction of Hsp70 expression suggested that Hsp90 inhibition by 17-AAG strongly activated HSF-1 (heat-shock transcription factor 1) (43). We also examined the levels of HCV core and NS5B protein expression in NNC#2 cells treated with 50 nM 17-AAG. Reduced levels of these proteins were seen in NNC#2 cells on day 6, and both HCV core and NS5B protein were undetectable on day 9 (Fig. 4*C*). To determine whether 17-AAG promoted the degradation of NS3, we next looked at the effect of 17-AAG on #50-1 cells in which proteasomal degradation was also inhibited. Although 17-AAG treatment still induced a reduction in the NS3 protein level in #50-1 cells (Fig. 4*D*), the degradation of NS3 was completely blocked in the presence of the proteasome inhibitor, MG132. This suggested that the pharmacological effect of 17-AAG was dependent on the proteasome system (44, 45).

Protein Folding in Hsp90-NS3 Interaction—To investigate the role of Hsp90 in HCV NS3 activation, the FLAG-NS3 protein was transfected into 293T cells, with or without 17-AAG, and the cell lysates were analyzed by Western blotting. The expression of NS3 from FLAG-NS3 was reduced in the presence of 17-AAG (Fig. 5*A*), suggesting that Hsp90 is involved in HCV NS3 degradation, possibly through a physical interaction.

We confirmed this specific interaction by immunoprecipitating 293T cell lysates with anti-FLAG antibody. This clearly showed that FLAG and Hsp90 co-precipitated, suggesting that NS3 was bound to the chaperone complex formed with Hsp90 (Fig. 5*B*). NS3 mutants lacking the protease and helicase regions were generated in order to identify the region responsible for the interaction with Hsp90 (Fig. 5*C*). FLAG-NS3, FLAG-NS3-Δhelicase, or FLAG-NS3-Δprotease were transfected into 293T cells, and anti-FLAG antibody immunoprecipitates were analyzed by Western blotting (Fig. 5*D*). Although FLAG-NS3-Δprotease was clearly co-immunoprecipitated with Hsp90, no protein band corresponding to FLAG-NS3-Δhelicase was detected (Fig. 5*D*), suggesting that the NS3 helicase region mediates binding to Hsp90. To confirm this finding, plasmids expressing different NS3 helicase mutants fused with FLAG (ΔPH 1, ΔPH 2, and ΔH 1) were constructed (Fig. 5*E*). Expressing these NS3 helicase mutants in 293T cells and analyzing their immunoprecipitates with anti-FLAG antibody by Western blotting showed that, although all of the NS3 helicase mutant proteins were immunoprecipitated by anti-FLAG-antibody, no Hsp90 was co-precipitated (Fig. 5*F*).

We also confirmed that the NS3 helicase region mediated the specific interaction with Hsp90 by transfecting FLAG-NS3 and FLAG-NS3 deletion mutants into 293T cells pretreated with 17-AAG (Fig. 5*G*). The proteins expressed by FLAG-NS3 and FLAG-NS3-Δprotease were degraded in cells pretreated with 17-AAG, whereas no degradation of the ΔPH 2 and ΔH 1 NS3 mutants lacking helicase regions was seen (Fig. 5*G*). Further, when pEF-core was expressed in 293T cells, core was unable to co-immunoprecipitate Hsp90, and no degradation of core protein was observed (Fig. 5*G*). Our data demonstrate that 17-AGG destabilizes several binding proteins (NS3 and NS3-Δprotease) to Hsp90 but stablilizes some nonbinding proteins (the ΔPH 2 and ΔH 1 NS3 mutants lacking helicase regions and core) to Hsp90. In previous reports (46), similar effects were observed when wild-type and mutated p53 were translated in the presence of geldanamycin. These results further supported the hypothesis that Hsp90 has a role in folding the NS3 helicase domain and that this has an important role in stabilizing the full-length NS3 protein. A protein complex that includes NS3 and Hsp90 is therefore implicated in the control of HCV replication.

DISCUSSION

The Hsp90 inhibitor, 17-AAG, is known to have highly selective effects on tumor cells that are a result of its high affinity for Hsp90 client oncoproteins, which are incorporated into the Hsp90-dependent multichaperone complex, thereby increasing their binding affinity for 17-AAG more than 100-fold (47). This high selectivity effectively minimizes the toxic side effects of 17-AAG so that it is a good candidate for clinical application, especially in treating neurodegenerative diseases. In this study, we observed the inhibitory effects of 17-AAG on the replication of an HCV subgenomic replicon that lacked NS2. On the other hand, Waxman *et al.* (37) demonstrated a role for Hsp90 in promoting the cleavage of HCV NS2/3 protein using NS2/3 translated in rabbit reticulocyte lysate and expressed in Jurkat cells. Because the replicon cells used in our study genetically lacked NS2, our results suggest that Hsp90 may directly interact with the NS3 protein in the HCV replicon.

In cell lines in which 17-AAG was a potent inhibitor of HCV replication, with IC_{50} values of 3–10 nM, we also found strong evidence that the association between HCV Hsp90 and NS3, but not other NS proteins, was the essential mechanism controlling the preferential degradation of NS3 after 17-AAG treatments. Furthermore, we showed that NS3 interacted with Hsp90 through the NS3 helicase domain. It was also clear that the expression of NS3 protein with helicase activity in 293T cells pretreated with 17-AAG was reduced, but the expression of NS3 mutants lacking the helicase regions (ΔPH 2 and ΔH 1) was not. The role of Hsp90 in achieving and/or stabilizing the NS3 protein was suggested by the fact that only 17-AGG bound to Hsp90 was capable of affecting NS3. The use of Hsp90 inhibitors represents a novel strategy for the development of anti-HCV therapies.

Acknowledgments—We are grateful to M. Sato, R. Tobita, and Y. Katumura for excellent technical assistance.

REFERENCES

1. Alter, H. J., Purcell, R. H., Shih, J. W., Melpolder, J. C., Houghton, M., Choo, Q. L., and Kuo, G. (1989) *N. Engl. J. Med.* **321,** 1494–1500
2. Choo, Q. L., Kuo, G., Weiner, A. J, Overby, L. R., Bradley, D. W., and Houghton, M. (1989) *Science* **244,** 359–362
3. McHutchison, J. G., Gordon, S. C., Schiff, E. R., Shiffman, M. L., Lee, W. M., Rustgi, V. K., Goodman, Z. D., Ling, M. H., Cort, S., and Albrecht, J. K. (1998) *N. Engl. J. Med.* **339,** 1485–1492
4. Glue, P., Rouzier-Panis, R., Raffanel, C., Sabo, R., Gupta, S. K., Salfi, M., Jacobs, S., and Clement, R. P. (2000) *Hepatology* **32,** 647–653
5. Saito, I., Miyamura, T., Ohbayashi, A., Harada, H., Katayama, T., Kikuchi, S., Watanabe, Y., Koi, S., Onji, M., and Ohtaet, Y. (1990) *Proc. Natl. Acad. Sci. U. S. A.* **87,** 6547–6549
6. Seeff, L. B. (1997) *Hepatology* **26,** 21S–28S
7. Bartenschlager, R., and Lohmann, V. (2001) *Antiviral Res.* **52,** 1–17
8. Taylor, D. R., Shi, S. T., Romano, P. R., Barber, G. N., and Lai, M. M. (1999) *Science* **285,** 107–110
9. Grakoui, A., Wychowski, C., Lin. C., Feinstone, S. M., and Rice, C. M. (1993) *J. Virol.* **67,** 1385–1395
10. Hijikata, M., Mizushima, H., Akagi, T., Mori, S., Kakiuchi, N., Kato, N., Tanaka, T., Kimura, K., and Shimotohno, K. (1993) *J. Virol.* **67,** 4665–4675
11. Grakoui, A., McCourt, D. W., Wychowski, C., Feinstone, S. M., and Rice, C. M. (1993) *Proc. Natl. Acad. Sci. U. S. A.* **90,** 10583–10587
12. Bartenschlager, R., Ahlborn-Laake, L., Mous, J., and Jacobsen, H. (1993) *J. Virol.* **67,** 3835–3844
13. Grakoui, A., McCourt, D. W., Wychowski, C., Feinstone, S. M., and Rice, C. M. (1993) *J. Virol.* **67,** 2832–2843
14. Bartenschlager, R., Lohmann, V., Wilkinson, T., and Koch, J. O. (1995) *J. Virol.* **69,** 7519–7528
15. Failla, C., Tomei, L., and De Francesco, F. (1995) *J. Virol.* **69,** 1769–1777
16. Lin, C., Thomson, J. A., and Rice, C. M. (1995) *J. Virol.* **69,** 4373–4380
17. Tanji, Y., Hijikata, M., Satoh, S., Kaneko, T., and Shimotohno, K. (1995) *J. Virol.* **69,** 1575–1581
18. Egger, D., Wolk, B., Gosert, R., Bianchi, L., Blum, H. E., Moradpour, D., and Bienz, K. (2002) *J. Virol.* **76,** 5974–5984
19. Gosert, R., Egger, D., Lohmann, V., Bartenschlager, R., Blum, H. E., Bienz, K., and Moradpour, D. (2003) *J. Virol.* **77,** 5487–5492
20. Blight, K. J., Kolykhalov, A. A., and Rice, C. M. (2000) *Science* **290,** 1972–1974
21. Guo, J. T., Bichko, V. V., and Seeger, C. (2001) *J. Virol.* **75,** 8516–8523
22. Krieger, N., Lohmann, V., and Bartenschlager, R. (2001) *J. Virol.* **75,** 4614–4624

23. Lohmann, V., Hoffmann, S., Herian, U., Penin, F., and Bartenschlager, R. (2003) *J. Virol.* **77,** 3007–3019
24. Behrens, S. E., Tomei, L., and De Francesco, R. (1996) *EMBO J.* **15,** 12–22
25. Lohmann, V., Korner, F., Herian, U., and Bartenschlager, R. (1997) *J. Virol.* **71,** 8416–8428
26. Friebe, P., and Bartenschlager, R. (2002) *J. Virol.* **76,** 5326–5338
27. Kolykhalov, A. A., Mihalik, K., Feinstone, S. M., and Rice, C. M. (2000) *J. Virol.* **74,** 2046–2051
28. Yanagi, M., St. Claire, M., Emerson, S. U., and Purcell Bukh, J. (1999) *Proc. Natl. Acad. Sci. U. S. A.* **96,** 2291–2295
29. Yi, M., and Lemon, S. M. (2003) *J. Virol.* **77,** 3557–3568
30. Picard, D. (2002) *Cell Mol. Life Sci.* **59,** 1640–1648
31. Wegele, H., Muller, L., and Buchner, J. (2004) *Rev. Physiol. Biochem. Pharmacol.* **151,** 1–44
32. Pratt, W. B., and Toft, D. O. (2003) *Exp. Biol. Med.* **228,** 111–133
33. Smith, D. F., Whitesell, L., and Katsanis, E. (1998) *Pharmacol. Rev.* **50,** 493–514
34. McClellan, A. J., and Frydaman, J (2001) *Nat. Cell Biol.* **3,** E1–E3
35. Grenert, J. P., Sullivan, W. P., Fadden, P., Haystead, T. A., Clark, J., Mimnaugh, E., Krutzsch, H., Ochel, H. J., Schulte, T. W., Sausville, E., Neckers, L. M., and Toft, D. O. (1997) *J. Biol. Chem.* **272,** 23843–23850
36. Supko, J. G., Hickman, R. L., Grever, M. R., and Malspeis, L. (1995) *Cancer Chemother. Pharmacol.* **36,** 305–315
37. Waxman, L., Whitney, M., Pollok, B. A., Kuo, L. C., and Darke, P. L. (2001) *Proc. Natl. Acad. Sci. U. S. A.* **98,** 13931–13935
38. Nakagawa, S., Umehara, T., Matsuda, C., Kuge, S., Sudoh, M., and Kohara, M. (2007) *Biochem. Biophys. Res. Commun.* **353,** 882–888
39. Okamoto, T., Nishimura, Y., Ichimura, T., Suzuki, K., Miyamura, T., Suzuki, T., Moriishi, K., and Matsuura, Y. (2006) *EMBO J.* **25,** 5015–5025
40. Kishine, H., Sugiyama, K., Hijikata, M., Kato, N., Takahashi, H., Noshi, T., Nio, Y., Hosaka, M., Miyanari, Y., and Shimotohno, K. (2002) *Biochem. Biophys. Res. Commun.* **290,** 993–999
41. Ishii, N., Watashi, K., Hishiki, T., Goto, K., Inoue, D., Hijikata, M., Wakita, T., Kato, N., and Shimotohno, K. (2006) *J. Virol.* **80,** 4510–4520
42. Takeuchi, T., Katsume, A., Tanaka, T., Abe, A., Inoue, K., Tsukiyama-kohara, K., Kawaguchi, R., Tanaka, S., and Kohara, M. (1999) *Gastroenterology* **11,** 636–642
43. Sittler, A., Lurz, R., Ueder, G., Priller, J., Lehrach, H., Hayer-Hartl, M. K., Hartl, F. U., and Wanker, E. E. (2001) *Hum. Mol. Genet.* **10,** 1307–1315
44. Bonvini, P., Dalla Rosa, H., Vignes, N., and Rosolen, A. (2004) *Cancer Res.* **64,** 3256–3264
45. Mimnaugh, E. G., Chavany, C., and Neckers, L. (1996) *J. Biol. Chem.* **271,** 22796–22801
46. Blagosklonny, M. V., Toretsky, J., Bohen, S., and Neckers L. (1996) *Proc. Natl. Acad. Sci. U. S. A.* **93,** 8379–8383
47. Kamal, A., Thao, L., Sensintaffar, J., Zhang, L., Boehm, M. F., Fritz, L. C., and Burrows, F. J. (2003) *Nature* **425,** 357–359

Gene Therapy (2008), 1–6

www.nature.com/gt

ORIGINAL ARTICLE

Baculovirus-mediated interferon alleviates dimethylnitrosamine-induced liver cirrhosis symptoms in a murine model

Y Nishibe[1,4], H Kaneko[1], H Suzuki[1,4], T Abe[2], Y Matsuura[2] and H Takaku[1,3]

[1]Department of Life and Environmental Science, Chiba Institute of Technology, Chiba, Japan; [2]Research Center for Emerging Infectious Diseases, Research Institute for Microbial Diseases, Osaka University, Osaka, Japan and [3]High Technology Research Center, Chiba Institute of Technology, Chiba, Japan

The wild-type baculovirus Autographa californica *multiple nuclear polyhedrosis virus (AcMNPV) infects a range of mammalian cell types* in vitro *but does not replicate in these cells. The current study investigated the* in vivo *effect of AcMNPV in the mouse model of liver cirrhosis induced by the mutagen dimethylnitrosamine. Intraperitoneal injection of AcMNPV induced an immune response. The baculovirus was taken up by the liver and spleen where it suppressed liver injury and fibrosis through the induction of interferons. This study presents the first evidence of the feasibility of using baculovirus to treat liver cirrhosis.*
Gene Therapy advance online publication, 27 March 2008; doi:10.1038/gt.2008.29

Keywords: *baculovirus; HCV; immune therapy; interferon; liver cirrhosis*

Introduction

Chronic infection by the hepatitis C virus (HCV) is a major cause of liver cirrhosis (LC) in Japan and some southern European countries, including Italy and Spain, and affects >3% of the population worldwide.[1] Infected individuals are a reservoir for new infections, and are at risk of developing LC and hepatocellular carcinoma. Consequently, HCV infection is the foremost reason for performing liver transplants.[2] Antiviral therapy consisting of peginterferon alfa-2a/ribavirin leads to a sustained response in only half of all patients infected with HCV genotypes 1 and 4,[3,4] resulting in the need to develop new antiviral therapies. In addition, the emergence of drug resistance in RNA virus infections emphasizes the requirement for multiple drug targets to limit viral escape.

The main characteristic of LC is fibrosis. The normal liver equilibrium of collagen synthesis and decomposition by liver cell proteases is well balanced. In damaged cells, collagen is secreted to form persistent scars, and excess secreted collagen is degraded. However, this balance is disrupted by chronic hepatic damage such as fibrosis, a result of wound healing after repeated hepatic injury and impaired degradation of excess collagen.[5] Following liver damage, inflammatory lymphatic cells infiltrate the liver parenchyma, and many hepatic cells undergo apoptosis, leading to the activation of Kupffer cells. Hepatic stellate cells (HSCs) proliferate, become activated and secrete large amounts of extracellular matrices (such as collagen, fibronectin and elastin). Sinusoidal endothelial cells lose their fenestrations, and continual cardiac contraction of HSCs increases the blood-flow resistance in the liver sinusoid. The reduction of secreted collagen to normal levels is therefore likely to limit the progression of liver cancer and may lead to a cure for hepatitis.

We recently reported that the activation of natural immunity in mice by intranasal preadministration of baculovirus has a life-prolonging effect against lethal doses of influenza virus.[6] Baculovirus also stimulates Toll-like receptor 9, which plays an important role in the activation of innate immunity.[7] Baculovirus infection activates tumor necrosis factor-α, interleukin (IL)-1α and IL-1β expression in primary hepatocyte cultures,[8] probably due to the presence of small numbers of Kupffer cells in the culture population,[9] while adenoviral vector expression of interferon (IFN)-α and IFN-γ in the liver of rats with hepatic fibrosis improves the symptoms of hepatic fibrosis.[10,11]

In the present study, we used a mouse model of hepatic fibrosis to investigate the therapeutic efficacy of the baculovirus *Autographa californica* multiple nuclear polyhedrosis virus (AcMNPV) on immune response induction, and the suppression of liver injury and fibrosis *in vivo*. The results of the present study provide the first evidence of the feasibility of using baculovirus to treat LC.

Correspondence: Professor H Takaku, Department of Life and Environmental Science and High Technology Research Center, Chiba Institute of Technology, 2-17-1 Tsudanuma, Narashino-shi, Chiba 275-0016 Japan.
E-mail: hiroshi.takaku@it-chiba.ac.jp
[4]These authors contributed equally to this work.
Received 5 July 2007; revised 7 February 2008; accepted 10 February 2008

Results

Establishment of a mouse hepatic fibrosis model

The mutagen dimethylnitrosamine (DMN) causes liver function disorders and cirrhosis. It is widely used in

experimental animals, such as rats and mice[10,12–14] to create a low-mortality and reproducible model of liver fibrosis[15–18] that is characterized in the early stages by centrilobular injury, followed by perivenular fibrosis and the formation of septa with the development of micronodular cirrhosis after 3 weeks of treatment. In this model, collagen accumulation is preceded by hepatic stem cell proliferation, which accumulates where fibrous septa will later appear,[19] and is associated with increased mRNA expression of types I, III and IV procollagen.[20]

In the present study, we observed that the body weight of DMN-treated mice was significantly reduced compared with controls after 3 weeks of treatment in all of the groups. To quantitatively assess liver fibrosis, we measured the serum levels of alanine transaminase (ALT) and aspartate transaminase (AST), and found that they increased in all of the DMN-administered groups, indicating liver damage (Figure 1a). DMN treatment also increased overall collagen synthesis (Figure 1b), and led to the collapse of parenchymal cells and the formation of regenerative nodules separated by extensive fibrous septa, which are similar to the characteristic pathologic changes observed in human LC (Figures 1c and d).

Effects of intraperitoneal baculovirus injection in mice with DMN-induced LC

To examine the efficiency of baculovirus-mediated immunotherapy, mice with DMN-induced LC were intraperitoneally injected with baculovirus. Although complement-resistant baculovirus can express inserted foreign genes *in vivo*,[21,22] it is not known whether wild-type baculovirus AcMNPV that is not expressed *in vivo* is capable of infecting mammalian tissues. The tissue tropism of AcMNPV was therefore examined by PCR analysis of DNA isolated from 10^7 plaque-forming unit

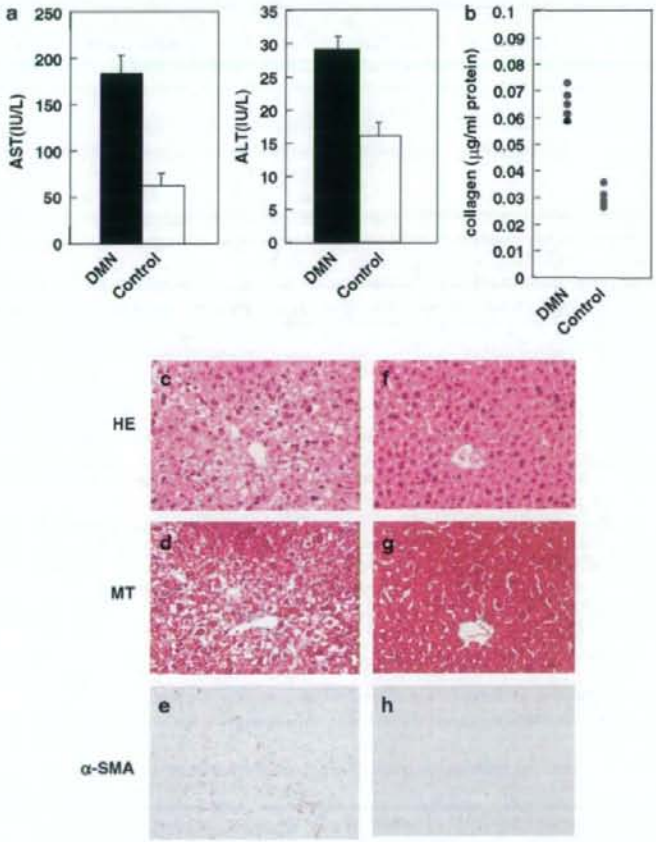

Figure 1 General effects of dimethylnitrosamine (DMN) treatment. (**a**) aspartate transaminase (AST, left) and alanine transaminase (ALT, right) determination of levels in mice treated with DMN (black bars) or control (white bars) for 3 weeks. (**b**) Collagen content of livers from mice treated with DMN for 3 weeks. (**c–g**) Hematoxylin and eosin (HE) and Masson's Trichrome (MT) staining of livers from mice treated with DMN (**c**, **d**) or saline (**f**, **g**) for 3 weeks. HE stains the nucleus blue and the cytoplasm pink, while MT stains collagen fibers blue, the cytoplasm pink and the nucleus dark purple. (**e**, **h**) Immunohistochemical staining of the liver using an anti-α-SMA antibody reveals extensive formation of fibrotic septa and thickened reticulin fibers joining central areas.

(PFU) AcMNPV-treated mice using AcMNPV-vp39-specific primers. The PCR products of the gp64 gene were predominantly detected in the liver and spleen following AcMNPV injection; no vp39 PCR products were detected following vehicle injection (Figure 2). A thin band representing vp39 was also detected in the lung (data not shown), which was probably infected by the pulmonary circulation.

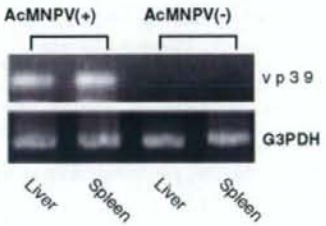

Figure 2 *In vivo Autographa californica* multiple nuclear polyhedrosis virus (AcMNPV) infectivity. Mice were injected with AcMNPV (10^7 PFU) or vehicle. After 48 h, tissues were harvested and total DNA was isolated. The AcMNPV genome was PCR-amplified using AcMNPV-vp39-specific primers. Data shown are from duplicate experiments.

Mice treated for 3 weeks with DMN were intraperitoneally injected with baculovirus (10^3, 10^5 and 10^7 PFU per 200 µl), lipopolysaccharide (LPS; 75 µg per 200 µl) or saline (200 µl) twice a day at 2-day intervals for 3 weeks. LPS was used as a control because inflammatory cytokines are reportedly induced after the administration of baculovirus. Histologic examination using hematoxylin and eosin (HE) staining revealed fewer fibrous connective tissue components in Glisson's sheath, and pseudolobule formations in the livers of control and baculovirus-administered mice compared with mice treated with DMN and saline. In mice treated with DMN, extensive formations of fibrotic septa and thickened reticulin fibers joining central areas were observed (Figures 1c, d and 3a–e). Masson's Trichrome (MT) staining revealed collagen in the bridging fibrous sinusoid of livers from saline-administered mice, whereas the livers from baculovirus-administered mice were almost devoid of collagen (Figures 3f–j). The expression of α-smooth muscle actin (α-SMA) was reduced in activated stellate cells of DMN-treated mice compared with those of mice treated with baculovirus (Figures 3k–n).

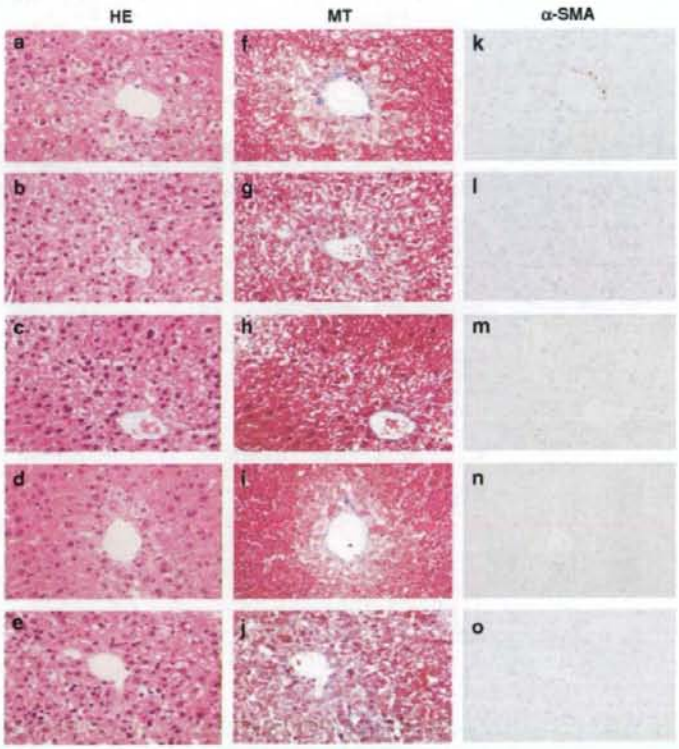

Figure 3 Alleviation of dimethylnitrosamine (DMN)-induced mouse liver cirrhosis (LC) following *Autographa californica* multiple nuclear polyhedrosis virus (AcMNPV) injection. Mice were treated with DMN then injected with saline (**a**, **f**, **k**), 10^3 AcMNPV (**b**, **g**, **l**), 10^5 AcMNPV (**c**, **h**, **m**), 10^7 AcMNPV (**d**, **i**, **n**) or 75 µg per 200 µl lipopolysaccharide (LPS, **e**, **j**, **o**). Liver sections were stained with hematoxylin and eosin (HE, **a**–**e**), Masson's Trichrome (MT, **f**–**j**) or an antibody against α-smooth muscle actin (α-SMA, **k**–**o**).

The levels of collagen in the liver were confirmed by colorimetry. Saline administration did not affect the extent of DMN-induced collagen accumulation, which remained high (Figure 4a). In contrast, administration of baculovirus significantly reduced the amount of accumulated collagen compared to the saline group, although there were no significant differences between different concentrations of baculovirus. We also used reverse transcription (RT)–PCR to examine the hepatic expression of AcMNPV-vp39 and revealed no significant differences between mice infected with different concentrations of AcMNPV (10^3, 10^5 and 10^7 PFU; Figure 4b). This may be due to the fact that *vp39* gene expression, which is associated with the instability of baculoviral DNA in mice, is independent of the viral dose. These results indicate that baculovirus administration alleviated hepatic tissue damage by decreasing the accumulation of collagen.

To quantitatively assess the extent of liver fibrosis, we measured the serum levels of AST and ALT. Baculovirus-administered mice had significantly lower levels of transaminases than DMN- or saline-injected mice (Figures 4c and d). As DMN-induced hepatic transaminase elevation does not regress spontaneously in the mouse LC model,[23–25] our observation suggested that baculovirus can rescue mice from DMN-induced hepatic damage and improve LC histopathology.

The expression of matrix metalloproteases (MMPs) and tissue inhibitors of metalloproteinases (TIMP), which is related to matrix degradation during liver fibrosis, was then analyzed by RT–PCR (Figure 5). Interstitial collagenase (MMP-13) is an essential enzyme for collagenolysis in liver fibrosis, and its expression increases at the peak of fibrosis development and drops rapidly during the recovery periods.[23,24] MMP-2, which is stimulated by transforming growth factor-β (TGF-β), is necessary for the proliferation and infiltration of HSCs during the process of fibrosis formation.[25–29] Increased TIMP-1 expression promotes liver fibrosis progression by preventing the degradation of secreted collagens, and TIMP-1 expression decreases during the recovery phase.[30] In this study, MMP-13, MMP-2 and TIMP-1 expression levels were downregulated in mouse livers treated with baculovirus compared with saline-injected cirrhotic livers (Figure 5).

IFN induction

IFN-γ has previously been shown to have immunomodulatory effects,[31] and decreases collagen synthesis in human chondrocytes, fetal rat bone and human dermal fibroblasts.[32–35] *In vivo* models of enhanced collagen synthesis have also revealed that IFN-γ reduces the collagen accumulation associated with foreign bodies, skin wound healing and bleomycin-induced lung

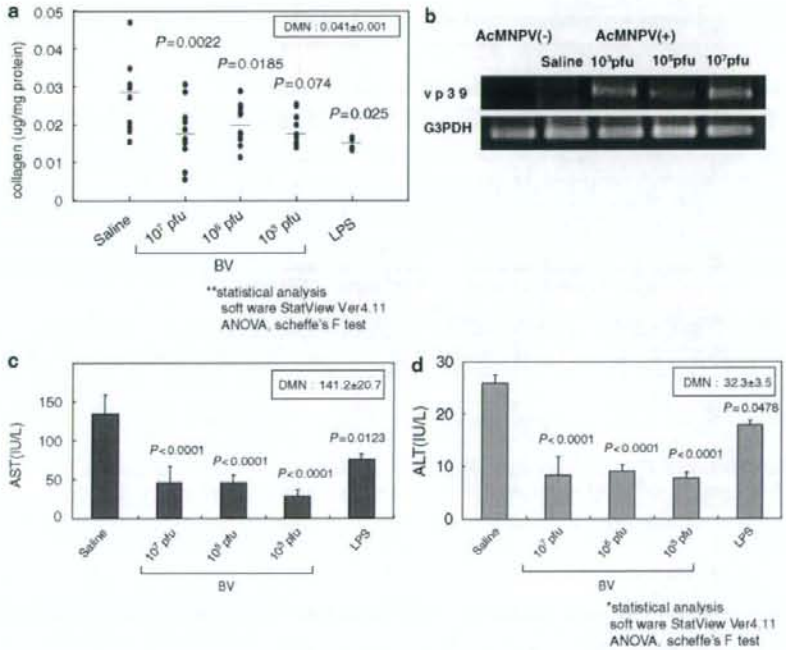

Figure 4 Markers of hepatic fibrosis and damage. Blood and liver tissues were collected 6 days after *Autographa californica* multiple nuclear polyhedrosis virus (AcMNPV) infection. (**a**) After treatment with dimethylnitrosamine (DMN) for 3 weeks, mice were infected with 10^3, 10^5 or 10^7 PFU AcMNPV (BV) or lipopolysaccharide (LPS). The hepatic collagen content was determined and compared with that of saline-treated livers. (**b**) Mice were intraperitoneally injected with baculovirus (10^3, 10^5 and 10^7 PFU per 200 µl) or saline and the AcMNPV genome was PCR-amplified using AcMNPV-vp39-specific primers. (**c**) Aspartate transaminase (AST) and (**d**) alanine transaminase (ALT) levels of DMN-treated mice injected with saline, AcMNPV or LPS, as before.

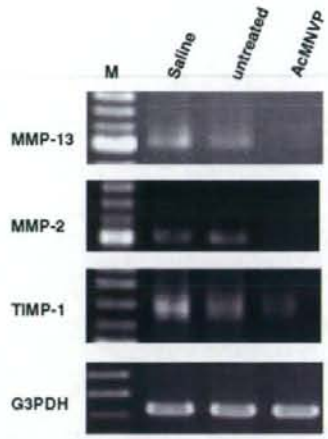

Figure 5 Hepatic matrix metalloproteases (MMPs) and tissue inhibitors of metalloproteinases (TIMP). MMP-13, MMP-2 and TIMP-1 mRNA levels were analyzed by reverse transcription (RT)–PCR in dimethylnitrosamine (DMN)-treated mice infected with 10^7 PFU per 200 μl *Autographa californica* multiple nuclear polyhedrosis virus (AcMNPV), saline, or left untreated.

fibrosis.[36–38] Further, in liver fibrosis induced by *Schistosoma mansoni* infection, IFN-γ significantly reduces collagen accumulation, and type I and III procollagen mRNA levels. Hepatocyte growth factor (HGF) is one of a potent growth factors involved in liver regeneration and has a strong effect on epithelial and nonepithelial cells.[39–42] On the other hand, it is reported that the overexpression of TGF-β plays a pivotal role in the progression of fibrosis.[43,44]

In the present study, hepatic expression levels of IFNs, HGF and TGF-β mRNAs were examined by RT–PCR (Figure 6). IFN-γ mRNA expression was observed 12, 24 and 48 h after the administration of baculovirus. Strong HGF expression was observed only 2 h after administration of the baculovirus, whereas TGF-β expression was reduced after 12 h. This finding suggests that HGF inhibits TGF-β expression.[45] HGF gene expression decreased after 12 h, and returned to untreated control levels after 48 h. These results indicate that IFNs and HGF are induced by baculovirus administration, and that these factors inhibit TGF-β, thereby alleviating hepatic fibrosis.

Discussion

In the present study, we established a mouse model of hepatic fibrosis using intraperitoneal administration of the mutagen DMN every second day for 3 weeks. Hepatic damage was monitored and confirmed by the presence of high serum levels of collagen and the transaminases ALT and ASL. Control saline administration did not alleviate the effects of DMN on the liver, as the collagen, ALT and ASL levels remained high. However, baculovirus administration significantly reduced the levels of collagen, ALT and ASL, although there was no significant difference between different baculovirus concentrations.

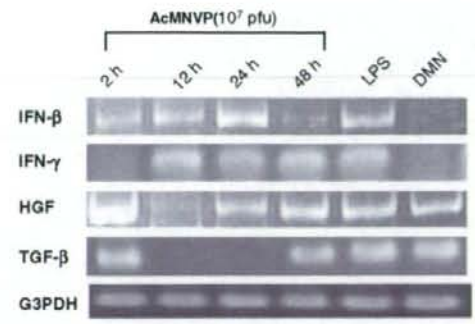

Figure 6 Hepatic interferons (IFNs), hepatocyte growth factor (HGF) and transforming growth factor-β (TGF-β). IFNs, HGF and TGF-β mRNA levels were analyzed by reverse transcription (RT)–PCR in dimethylnitrosamine (DMN)-treated mice infected with 10^7 PFU per 200 μl *Autographa californica* multiple nuclear polyhedrosis virus (AcMNPV) or lipopolysaccharide (LPS).

Collagen levels were measured to evaluate the effect of baculovirus on the hepatic accumulation of collagen, another indicator of DMN-induced hepatitis. Compared to saline administration, baculovirus administration significantly decreased the accumulation of collagen, although there were no statistical differences among different baculovirus concentrations. The improvement in the formation of collagen fibers induced by baculovirus administration was analyzed pathologically by MT staining. The expression of α-SMA was reduced in the activated stellate cells of mice that were administered with baculovirus. Although DMN-induced fiber formation in the sinusoid was not improved after the administration of saline, fibrosis was alleviated by the administration of baculovirus. Moreover, alleviation of fibrosis correlated with the level of collagen.

The examination of hepatic cells by HE staining revealed marked centrolobular vacuole degeneration after DMN administration, which was not improved by saline administration. However, baculovirus administration alleviated the degeneration in a dose-dependent manner.

During the progression of liver fibrosis, there is a marked increase in TIMPs, which leads to a net decrease in the catalytic activity of MMPs. Evaluation of the expression of these key molecules in the present study revealed that the steady-state level of mRNA transcripts for interstitial collagenase MMPs following administration of baculovirus was lower compared with that in saline-injected cirrhotic animals. Hepatic regeneration is an important component of the recovery process that occurs after various hepatic injuries.[46] Previous studies of liver regeneration following acute liver damage or partial hepatectomy demonstrated that the hepatic biomatrix contains large amounts of HGF,[47] predominantly around portal triads.[48] Matrix breakdown may cause rapid release of HGF, thus accounting for the rapid increase in HGF levels in the blood plasma. In the present study, HGF levels were increased in baculovirus-administered animals, correlating with increased HGF mRNA and protein expression. RT–PCR revealed strong HGF expression after only 2 h, and a reduction in the

expression of TGF-β after 12 h. This finding suggests that HGF was overexpressed during baculovirus infection, and that the resultant HGF protein inhibited TGF-β expression. Baculovirus infection also induced the expression of IFNs, indicating that the effects of the baculovirus in a mouse model of DMN-induced hepatic fibrosis are mediated by the downregulation of collagen and MMPs, and the upregulation of HGF.

In conclusion, we have demonstrated that intraperitoneal inoculation with the baculovirus AcNPV alleviates hepatic fibrosis and improves hepatic damage in a mouse model of DMN-induced hepatic fibrosis. The present study, to our knowledge, is the first to provide evidence of the feasibility and advantages of using baculovirus to treat HCV-associated liver diseases.

Materials and methods

Purified wild-type AcMNPV

Wild-type baculovirus AcMNPV was purchased from BD Biosciences (San Diego, CA, USA). Sf-9 insect cells were cultured at 27 °C in Sf-900IISFM (Invitrogen Corp., Carlsbad, CA, USA) containing 10% fetal bovine serum and 100 μg ml $^{-1}$ kanamycin sulfate. Purification of the baculovirus was performed as previously described.[12] The virus stocks were endotoxin free (<0.01 U ml $^{-1}$), as determined by a Pyrodick endotoxin measurement kit (Seikagaku Co., Tokyo, Japan).

Experimental design

A total of 55 female 7-week-old BALB/c mice (Charles River, Tokyo, Japan) were housed in plastic cages with a wire mesh base providing isolation from a hygienic bed, and were exposed to a 12 h controlled light cycle. Experiments were performed in accordance with institutional ethical guidelines. Hepatic fibrosis was induced by intraperitoneal injections of 10 mg kg $^{-1}$ DMN (Sigma, St Louis, MO, USA) dissolved in saline to obtain a 1% solution, which was administered on 3 consecutive days a week for 3 weeks.

After the DMN injections, five mice were killed to examine LC development. The remaining 50 mice received intraperitoneal injections of a single infusion of 200 μl saline ($n=10$), 10^5 PFU AcMNPV ($n=10$), 10^5 PFU AcMNPV ($n=10$), 10^7 PFU AcMNPV ($n=10$) or 75 μg LPS ($n=10$).

Body and liver weights were recorded (data not shown), and blood samples were obtained for routine ALT and AST determination.

PCR and analysis of amplified products

Total DNA was purified from various tissues, and the presence of AcMNPV (10^7 PFU) was detected by performing PCR amplification of the viral gene AcMNPV-vp39. The sequences of the specific primers were as follows: AcMNPV-vp39, 5′-TATGGCGCCGCG ACAAATGAGAGTT-3′ (sense) and 5′-TTCGCCTGCAA CACCAGGCGCAGG-3′ (antisense); glyceraldehyde-3-phosphate dehydrogenase (G3PDH), 5′-TCCACCACC CTGTTGCTGTA-3′ (sense) and 5′-ACCACAGTCCAT GCCATCAC-3′ (antisense). After RT, nest PCR was performed to test the RT efficiency. Nest PCR were all assembled in 10 μl, including 1 μl first round PCR products as template for second PCR, 0.2 μl, 0.02 μM sense primer, 0.2 μl, 0.02 μM antisense primer, 2 μl, 10 × PCR buffer with deoxyribonucleotide triphosphate AmpliTaq Gold (Applied Biosystems Co. Ltd, Foster City, CA, USA), 0.1 μl AmpliTa Gold DNA polymerase (Applied Biosystems Co. Ltd) and $MgCl_2$. The RT–PCR products were amplified using the following thermal cycle program: 95 °C for 10 min, 30 cycles of 94 °C for 1 min, X °C for Y min and 72 °C for 1 min, followed by 72 °C for 7 min. PCR products were electrophoresed on 1.5% agarose gels. The sequences of the specific primers were as follows: AcMNPV-vp39, 5′-GACTGCGCCGCCG CCCAGAGTAGCGTTAGG-3′ (sense) and 5′-CTGCATT TTCGCGTCCATCGTGTCGTTCGA-3′ (antisense).

Tissue preparation

Liver specimens were routinely fixed in 4% phosphate-buffered formaldehyde or methanol for 18–24 h and were then embedded in paraffin. Tissue sections (4 mm thickness) were stained with HE for routine examination or with MT for collagen visualization and morphometric analysis.

For RNA extraction, one-half of the remaining liver was cut into 150 mg pieces, dipped in liquid nitrogen and stored at −80 °C until required. The remaining liver tissue was finely minced and homogenized in three volumes of ice-cold buffer (50 mmol l $^{-1}$ Tris, 150 mmol l $^{-1}$ KCl, 1 mmol l $^{-1}$ ethylene diamine tetra-acetic acid (pH 7.4)).

RT–PCR

Total RNA was isolated from 150 mg liver specimens using the Isogen reagent (Nippon Gene, Tokyo, Japan). RT–PCR was performed with 2 μg RNA and the Takara One-Step RNA PCR Kit (Takara Bio Inc., Shiga, Japan). The forward primers were as follows: TGF-β, 5′-CG GGGCGACCTGGGCACCATCCATGAC-3′; HGF, 5′-CC GAGGCCATGGTGCTACA-3′; IFN-α, 5′-GACTCATCT GCTGCTTGGAATGCAACCCTC-3′; IFN-β, 5′-ATGAAC AACAGGTGGATCCTCCSCGCTG-3′ and IFN-γ, 5′-AGC GGCTGACTGAACTCAGATTGTAG-3′. The reverse primers were as follows: TGF-β, 5′-CTGCTCCACCTTG GGTTGCGACCCAC-3′; HGF, 5′-CTCGGATGTTTGGGT CAGTTG-3′; IFN-α, 5′-GACTCACTCCTTCTCCTCAGT CTTGCC-3′; IFN-β, 5′-TCAGTTTTGGAAGTTTCTGGTA AGTCTTCG-3′ and IFN-γ, 5′-GTCACAGTTTTCAGCTG TATAGGG-3′. As an internal control, human G3PDH mRNA was amplified simultaneously with primers G3PDH-F (nucleotides 230–254) and downstream G3PDH-R (nucleotides 422–466), generating a 0.5 kb product. The RT–PCR products were amplified using the following thermal cycle program: 42 °C for 60 min, 94 °C for 2 min, then 30 cycles of 94 °C for 1 min, T °C for 1 min and 72 °C for 1 min, followed by 72 °C for 10 min. PCR products were electrophoresed on 1.5% agarose gels.

Colorimetric measurement of collagen

Briefly, at least five 15 μm thick sections from three samples per animal were deparaffinized, placed in 0.5 M acetic acid and homogenized. After centrifugation, the supernatant was treated with Sircol Collagen Assay Kit Dye Reagent (Biocolor Ltd, Belfast, UK) according to the manufacturer's instructions. After washing with distilled water, both dyes were eluted using an alkali reagent. The absorbance obtained at 540 nm was determined to

calculate the amount of collagen in each section (expressed as μg total collagen per mg total protein).

Immunohistochemical examination

Immunohistochemical analysis was performed using an antibody against mouse α-SMA (GeneTex Inc., San Antonio, TX, USA).

MMPs and TIMP expression

Levels of MMP-13, MMP-2 and TIMP-1 expression were examined by RT–PCR as described above using the following primer sets: MMP-13, forward (5′-TGACT ATGCGATGGCTGGAA-3′) and reverse (5′-AAGCTGA AATCTTGCCTTGGA-3′; 355 bp); MMP-2, forward (5′-A CCATCGCCCATCATCAAGT-3′) and reverse (5′-CGAG CAAAAGCATCATCCAC-3′; 348 bp); TIMP-1, forward (5′-CCGCAGACGGCGTTCT-GCAA-3′) and reverse (5′-T CGAGACCCAAGGGATTGCC-3′; 525 bp). In total, 35 cycles (or 30 cycles for MMP-2) of PCR were carried out at 94 °C for 30 s, at 58 °C (or 52 °C for MMP-13) for 30 s and at 72 °C for 30 s, and the PCR products were electrophoresed on 2% agarose gels.

Statistical analysis

Survival of rats was determined by the Kaplan–Meier method and compared by the logrank test. The difference in experimental parameters and proliferation indices among the treatment groups was analyzed using the one-way analysis of variance test. For all tests, $P<0.05$ was considered significant.

Acknowledgements

This work was supported, in part, by a grant from the Research and Development Program for New Bio-industry Initiatives and by a Grant-in-Aid for High Technology Research, no. 09309011, from the Ministry of Education, Science, Sports, and Culture, Japan.

References

1 World Health Organization. Hepatitis C: global prevalence. *Wkly Epidemiol Rec* 1997; **72**: 341–344.
2 Fishman JA, Rubin RH, Koziel MJ, Periera BJ. Hepatitis C virus and organ transplantation. *Transplantation* 1996; **62**: 147–154.
3 Heathcote EJ, Shiffman ML, Cooksley WG, Dusheiko GM, Lee SS, Balart L *et al*. Peginterferon alfa-2a in patients with chronic hepatitis C and cirrhosis. *N Engl J Med* 2000; **343**: 1673–1680.
4 Zeuzem S, Feinman SV, Rasenack J, Heathcote EJ, Lai MY, Gane E *et al*. Peginterferon alfa-2a in patients with chronic hepatitis C. *N Engl J Med* 2000; **343**: 1666–1672.
5 Bataller R, Brenner DA. Liver fibrosis. *J Clin Invest* 2005; **115**: 209–218.
6 Abe T, Takahashi H, Hamazaki H, Miyano-Kurosaki N, Matsuura Y, Takaku H. Baculovirus induces an innate immune response and confers protection from lethal influenza virus infection in mice. *J Immunol* 2003; **171**: 1133–1139.
7 Abe T, Hemmi H, Moriishi K, Tamura S, Takaku H, Akira S *et al*. Involvement of the Toll-like receptor 9 signaling pathway in the induction of innate immunity by baculovirus. *J Virol* 2005; **79**: 2847–2858.
8 Gronowski AM, Hilbert DM, Sheehan KC, Garotta G, Schreiber RD. Baculovirus stimulates antiviral effect in mammalian cells. *J Virol* 1999; **73**: 9944–9951.
9 Beck NB, Sidhu JS, Omiecinski CJ. Baculovirus vectors repress phenobarbital-mediated gene induction and stimulate cytokine expression in primary cultures of rat hepatocytes. *Gene Therapy* 2000; **7**: 1274–1283.
10 Baroni GS, D'Ambrosio L, Curto P, Casini A, Mancini R, Jezequel AM *et al*. Interferon gamma decreases hepatic stellate cell activation and extracellular matrix deposition in rat liver fibrosis. *Hepatology* 1996; **23**: 1189–1199.
11 Suzuki K, Aoki K, Ohnami S, Yoshida K, Kazui T, Kato N *et al*. Adenovirus-mediated gene transfer of interferon a improves dimethylnitrosamine-induced liver cirrhosis in rat model. *Gene Therapy* 2003; **10**: 765–773.
12 Kitamura K, Nakamoto Y, Akiyama M, Fujii C, Kondo T, Kobayashi K *et al*. Pathogenic roles of tumor necrosis factor receptor p55-mediated signals in dimethylnitrosamine-induced murine liver fibrosis. *Lab Invest* 2002; **82**: 571–583.
13 Jenkins SA, Grandison A, Baxter JN, Day DW, Taylor I, Shields R. A dimethylnitrosamine-induced model of cirrhosis and portal hypertension in the rat. *J Hepatol* 1985; **1**: 489–499.
14 Jezequel AM, Ballardini G, Mancini R, Paolucci F, Bianchi FB, Orlandi F. Modulation of extracellular matrix components during dimethylnitrosamine-induced cirrhosis. *J Hepatol* 1990; **11**: 206–214.
15 Tsukamoto H, Matsuoka M, French SW. Experimental models of hepatic fibrosis: a review. *Semin Liver Dis* 1990; **10**: 56–65.
16 Ramadori G. The stellate cell of the liver. New insights into pathophysiology of an intriguing cell. *Virchows Archiv B Cell Pathol Incl Mol Pathol* 1991; **61**: 147–158.
17 Fernandez-Munoz D, Caramelo C, Santos JC. Systemic and splanchnic hemodynamic disturbances in conscious rats with experimental liver cirrhosis without ascites. *Am J Physiol* 1985; **249**: G316–G320.
18 Baraona E, Liu W, Ma X-L, Svegliati Baroni G, Lieber CS. Acetaldehyde-collagen adducts in *N*-nitrosodimethylamine-induced liver cirrhosis. *Life Sci* 1993; **52**: 1249–1255.
19 Mancini R, Jezequel AM, Benedetti A, Paolucci F, Trozzi L, Orandi F. Quantitative analysis of proliferating sinusoidal cells in dimethylnitrosamine-induced cirrhosis. An immunohistochemical study. *J Hepatol* 1992; **15**: 361–366.
20 Ala-Kokko L, Pihlajaniemi T, Myers CJ, Kivirikko KI, Savo-lainen ER. Gene expression of type I, III and IV collagens in hepatic fibrosis induced by dimethylnitrosamine in the rat. *Biochem J* 1987; **244**: 75–79.
21 Hofmann C, Strauss M. Baculovirus-mediated gene transfer in the presence of human serum or blood facilitated by inhibition of the complement system. *Gene Therapy* 1998; **5**: 531–536.
22 Hüser A, Rudolph M, Hofmann C. Incorporation of decay-accelerating factor into the baculovirus envelope generates complement-resistant gene transfer vectors. *Nat Biotechnol* 2001; **19**: 451–455.
23 Jézéquel AM, Mancini R, Rinaldesi ML, Macarri G, Venturini C, Orlandi F. A morphological study of the early stages of hepatic fibrosis induced by low doses of dimethylnitrosamine in the rat. *J Hepatol* 1987; **5**: 174–181.
24 Fujimoto J, Kaneda Y. Reversing liver cirrhosis: impact of gene therapy for liver cirrhosis. *Gene Therapy* 1999; **6**: 305–306.
25 Lee HS, Huang GT, Miau LH, Chiou LL, Chen CH, Sheu JC. Expression of matrix metalloproteinases in spontaneous regression of liver fibrosis. *Hepatogastroenterology* 2001; **48**: 1114–1117.
26 Watanabe T, Niioka M, Hozawa S, Kameyama K, Hayashi T, Arai M *et al*. Gene expression of interstitial collagenase in both progressive and recovery phase of rat liver fibrosis induced by carbon tetrachloride. *J Hepatol* 2000; **33**: 224–235.
27 Overall CM, Wrana JL, Sodek J. Transcriptional and posttranscriptional regulation of 72-kDa gelatinase/type IV collagenase by

transforming growth factor-beta 1 in human fibroblasts. Comparisons with collagenase and tissue inhibitor of matrix metalloproteinase gene expression. *J Biol Chem* 1991; **266**: 14064–14071.

28 Poncelet AC, Schnaper HW. Regulation of human mesangial cell collagen expression by transforming growth factor-beta 1. *Am J Physiol* 1998; **275**: F458–F466.

29 Ikeda K, Wakahara T, Wang YQ, Kadoya H, Kawada N, Kaneda K. *In vitro* migratory potential of rat quiescent hepatic stellate cells and its augmentation by cell activation. *Hepatology* 1999; **29**: 1760–1767.

30 Iredale JP, Benyon RC, Arthur MJ, Ferris WF, Alcolado R, Winwood PJ *et al*. Tissue inhibitor of metalloproteinase-1 messenger RNA expression is enhanced relative to interstitial collagenase messenger RNA in experimental liver injury and fibrosis. *Hepatology* 1996; **24**: 176–184.

31 Powrie F, Coffman RL. Cytokine regulation of T-cell function: potential for therapeutic intervention. *Immunol Today* 1993; **14**: 270–274.

32 Czaja MJ, Weiner FR, Eghbali M, Giambrone MA, Zern MA. Differential effects of gamma-interferon on collagen and fibronectin gene expression. *J Biol Chem* 1987; **262**: 13348–13351.

33 Goldring MB, Sandell LJ, Stephenson ML, Krane SM. Immune interferon suppresses levels of procollagen mRNA and type III collagen synthesis in cultured human articular and costal chondrocytes. *J Biol Chem* 1986; **261**: 9049–9055.

34 Smith DD, Gowen M, Mundy GR. Effects of interferon-gamma and other cytokines on collagen synthesis in fetal rat bones cultures. *Endocrinology* 1987; **120**: 2494–2499.

35 Jimenez SA, Freundlich B, Rosenbloom J. Selective inhibition of human diploid fibroblast collagen synthesis by interferons. *J Clin Invest* 1984; **74**: 1112–1116.

36 Granstein RD, Murphy GF, Margolis RJ, Byrne MH, Amento EP. Gamma interferon inhibits collagen synthesis *in vivo* in the mouse. *J Clin Invest* 1987; **79**: 1254–1258.

37 Granstein RD, Deak MR, Jacques SL, Margolis RJ, Flotte TJ, Whitaker D *et al*. The systemic administration of gamma interferon inhibits collagen synthesis and acute inflammation in a murine skin wounding model. *J Invest Dermatol* 1989; **93**: 18–27.

38 Hyde DM, Henderson TS, Giri SN, Tyler NK, Stovall MY. Effect of murine gamma interferon on the cellular response to bleomycine in mice. *Exp Lung Res* 1988; **14**: 687–704.

39 Brinkmann V, Foroutan H, Sachs M, Weidner KM, Birchmeier W. Hepatocyte growth factor/scatter factor induces a variety of tissue-specific morphogenic programs in epithelial cells. *J Cell Biol* 1995; **131**: 1573–1586.

40 Kountouras J, Boura P, Lygidakis NJ. Liver regeneration after hepatectomy. *Hepatogastroenterology* 2001; **48**: 556–562.

41 Laurent S, Otsuka M, De Saeger C, Maiter D, Lambotte L, Horsmans Y. Expression of presumed specific early and late factors associated with liver regeneration in different rat surgical models. *Lab Invest* 2001; **81**: 1299–1307.

42 Wang H, Zhang Y, Heuckeroth RO. Tissue-type plasminogen activator deficiency exacerbates cholestatic liver injury mice. *Hepatology* 2007; **45**: 1527–1537.

43 Bissell DM, Roulot D, George J. Transforming growth factor β and the liver. *Hepatology* 2001; **34**: 859–867.

44 Gressner AM, Weiskirchen R, Breitkopf K, Dooley S. Roles of TGF-β in hepatic fibrosis. *Front Biosci* 2002; **7**: d793–d807.

45 Wiercinska E, Wickert L, Denecke B, Said HM, Hamzavi J, Gressner AM *et al*. Id1 is a critical mediator in TGF-β-induced transdifferentiation of rat hepatic stellate cells. *Hepatology* 2006; **43**: 1032–1041.

46 Bucher NLR. Regeneration of mammalian liver. *Int Rev Cytol* 1963; **15**: 245–300.

47 Masumoto A, Yamamoto N. Sequestration of a hepatocyte growth factor in extracellular matrix in normal adult rat liver. *Biochem Biophys Res Commun* 1991; **174**: 90–95.

48 Liu ML, Mars WM, Zarnegar R, Michalopoulos GK. Uptake and distribution of hepatocyte growth factor in normal and regenerating adult rat liver. *Am J Pathol* 1994; **144**: 129–140.

ELSEVIER
Journal of Hepatology xxx (2009) xxx–xxx
Journal of Hepatology
www.elsevier.com/locate/jhep

HCV replication suppresses cellular glucose uptake through down-regulation of cell surface expression of glucose transporters☆

Daisuke Kasai[1,†], Tetsuya Adachi[1,†], Lin Deng[1], Motoko Nagano-Fujii[1], Kiyonao Sada[1], Masanori Ikeda[2], Nobuyuki Kato[2], ~~Yoshihiro~~ Ide[1], Ikuo Shoji[1], Hak Hotta[1,*]

[1]*Divisions of Microbiology, Kobe University Graduate School of Medicine, 7-5-1 Kusunoki-cho, Chuo-ku, Kobe 650-0017, Japan*
[2]*Department of Molecular Biology, Okayama University Graduate School of Medicine and Dentistry, Okayama 700-8558, Japan*

***Background/Aims*: Persistent infection with hepatitis C virus (HCV) causes extrahepatic diseases, including diabetes. We investigated the possible effect(s) of HCV replication on cellular glucose uptake and expression of the facilitative glucose transporter (GLUT) 2 and 1.**

***Methods*: We used Huh-7.5 cells harboring either an HCV subgenomic RNA replicon (SGR) or an HCV full-genomic RNA replicon (FGR), HCV-infected cells, and the respective cells treated with interferon (IFN). We also used liver tissue samples obtained from patients with or without HCV infection.**

***Results*: Glucose uptake and surface expression of GLUT2 and GLUT1 were suppressed in SGR, FGR and HCV-infected cells compared to the control cells. Expression levels of GLUT2 mRNA, but not GLUT1 mRNA, were lower in SGR, FGR and HCV-infected cells than in the control. Luciferase reporter assay demonstrated decreased GLUT2 promoter activities in SGR, FGR and HCV-infected cells. IFN treatment restored glucose uptake, GLUT2 surface expression, GLUT2 mRNA expression and GLUT2 promoter activities. Also, GLUT2 expression was reduced in hepatocytes of liver tissues obtained from HCV-infected patients.**

***Conclusions*: HCV replication down-regulates cell surface expression of GLUT2 partly at the transcriptional level, and possibly at the intracellular trafficking level as suggested for GLUT1, thereby lowering glucose uptake by hepatocytes.**

***Keywords*: Diabetes mellitus; Down-regulation; Glucose uptake; GLUT1; GLUT2; Hepatitis C virus; Hepatocyte; Interferon; Replicon**

1. Introduction

Hepatitis C virus (HCV) is a small, enveloped RNA virus, which belongs to the genus *Hepacivirus* within the family *Flaviviridae*. The viral genome consists of single-stranded, positive-sense RNA of 9.6 kb that encodes a polyprotein of about 3000 amino acids. There are six major genotypes of HCV worldwide, with each genotype being further classified into a number of subtypes, such as HCV-1a and -1b [1,2]. The polyprotein is processed by host cellular and viral proteases to yield at least 10 structural and nonstructural (NS) proteins, such as core protein, envelope glycoproteins (E1 and E2), p7, NS2, NS3, NS4A, NS4B, NS5A and NS5B [3,4].

Received 15 June 2008; received in revised form 19 November 2008; accepted 11 December 2008
Associate Editor: F. Zoulim

☆ The authors who have taken part in the research of this paper declared that they do not have a relationship with the manufacturers of the materials involved either in the past or present and they did not receive funding from the manufacturers to carry out their research.

* Corresponding author. Tel.: +81 78 382 5500; fax: +81 78 382 5519.
E-mail address: hotta@kobe-u.ac.jp (H. Hotta).
† These authors contributed equally to this study.

Abbreviations: FGR, full-genome RNA replicon; GLUT, glucose transporter; HBV, hepatitis B virus; HCV, hepatitis C virus; IFN, interferon; SGR, subgenomic RNA replicon.

0168-8278/$34.00 © 2009 Published by Elsevier B.V. on behalf of the European Association for the Study of the Liver.
doi:10.1016/j.jhep.2008.12.029

Please cite this article in press as: Kasai D et al., HCV replication suppresses cellular glucose uptake through ..., J Hepatol (2009), doi:10.1016/j.jhep.2008.12.029

HCV prevails in most parts of the world with an estimated number of about 170 million carriers and, hence, HCV infection is a major global health-care problem [5]. Persistent infection with HCV causes not only liver diseases, including hepatitis, but also extrahepatic manifestations, such as type 2 diabetes [6–8]. While it has been known that liver cirrhosis impairs the glucose metabolism of the liver, there are some reports showing that HCV-infected patients of over 40 years old have an increased risk for type 2 diabetes three times higher than that for patients without HCV infection [9,10]. These reports imply the possibility that HCV infection directly predisposes the host toward type 2 diabetes. However, the precise mechanism(s) is poorly understood.

Glucose is transported into the cell via various isoforms of the facilitative glucose transporter (GLUT) that are present in most cells. Currently, a total of 14 isoforms have been identified in the GLUT family [11–13]. GLUT2 is expressed tissue-specifically in the liver, pancreatic β-cells, hypothalamic glial cells, retina and enterocytes [14]. On the other hand, GLUT1 is expressed at high levels in all fetal tissues and, in adult, it is widely expressed but most abundant in erythrocytes, endothelial cells of the blood–brain barrier, renal tubules of the kidney, and any kind of malignant cells including hepatocellular carcinoma [13].

In the present study, we demonstrated that HCV infection suppressed hepatocytic glucose uptake through down-regulation of surface expression of GLUT in a human hepatocellular carcinoma-derived cell line Huh-7.5. We also demonstrated that GLUT2 expression in hepatocytes of the liver tissues from HCV-infected patients was lower than in those from patients without HCV infection. We propose that HCV replication decreases glucose uptake and cell surface expression of GLUT, which would eventually lead to glucose metabolism disorder.

2. Materials and methods

2.1. Cell culture, HCV RNA replication, HCV infection and IFN treatment

A human hepatoma-derived cell line, Huh-7.5, which is highly permissive to HCV RNA replication [15], was kindly provided by Dr. C.M. Rice (The Rockefeller University, New York, NY, USA). The cells were maintained in Dulbecco's modified Eagle's medium supplemented with 10% heat-inactivated fetal calf serum.

Huh-7.5 cells stably harboring an HCV-1b subgenomic RNA replicon (referred to as SGR cells, hereafter) were prepared as describe previously [16–18], using pFK5B/2884Gly (a kind gift from Dr. R. Bartenschlager, University of Heidelberg, Heidelberg, Germany). In SGR cells, the HCV subgenomic RNA replicon autonomously replicates to express NS3 to NS5B of HCV (Fig. 1). Cells harboring a full-length HCV-1b RNA replicon derived from pON/C-5B (referred to as FGR cells, hereafter) were described previously [19,20]. In FGR cells, the genome-size HCV RNA replicon autonomously replicates to express all the HCV proteins (the core protein, E1, E2, p7, NS2, NS3 to NS5B).

The pFL-J6/JFH1 plasmid that encodes the entire viral genome of a chimeric strain of HCV-2a, J6/JFH1 [21], was kindly provided by Dr. C.M. Rice. The HCV RNA genome was transcribed *in vitro* from pFL-J6/JFH1 and transfected to Huh-7.5 cells. The virus produced in the culture supernatant was used for infection experiments at multiplicities of infection of 1.0 and cultured for 5 days after virus infection.

In some experiments, SGR and FGR cells, as well as HCV-infected cells at 5 days after virus infection, were treated with 1000 IU/ml of IFN (Sigma, St. Louis, MI, USA) for 10 days to eliminate HCV replication.

2.2. Immunofluorescence

Cells were fixed with 3.7% paraformaldehyde and incubated with mouse monoclonal antibody against HCV NS5A (Chemicon International, Inc., Temecula, CA, USA) or HCV core (Abcam, Tokyo, Japan). The cells were then incubated with fluorescein isothiocyanate (FITC)-conjugated goat anti-mouse IgG (MBL Co. Ltd., Nagoya, Japan), and observed under a fluorescent microscope (BX51; Olympus, Tokyo, Japan).

2.3. Immunoblotting

Cells were solubilized in lysis buffer as reported previously [22]. The cell lysates were electrophoresed subjected to 8% polyacrylamide gel electrophoresis and transferred to polyvinylidene difluoride membrane (Millipore Corp., Billerica, MA, USA). The membranes were incubated with mouse monoclonal antibodies against HCV NS5A or NS3 (Chemicon), followed by incubation with peroxidase-conjugated goat anti-mouse IgG (MBL). The positive bands were visualized by using ECL detection system (GE Healthcare UK Ltd., Buckinghamshire, UK).

2.4. Uptake of 2-deoxy-D-glucose and thymidine

Cells cultured in 12-well plates were deprived of serum by incubation in serum-free medium for 12 h. The cells were then pre-incubated for 20 min in 450 μl of KRH (25 mM Hepes, 120 mM NaCl, 5 mM KCl, 1.2 mM $MgSO_4$, 1.3 mM $CaCl_2$, 1.3 mM KH_2PO_4 and 0.1% BSA, pH 7.4). Glucose uptake assay was performed as describe previously [23]. In brief, glucose uptake was initiated by addition of 50 μl of reaction solution (KRH containing 0.5 mM, 0.25 μCi 2-deoxy-D-[1,2-^{3}H]glucose) to each well. As a negative control, 100 μM phloretin was added to reaction solution. After 10 min, transport was terminated by washing the cells with ice-cold KRH buffer containing 100 μM phloretin. The cells were solubilized by 0.1% sodium dodecyl sulfate, and the incorporated radioactivity was measured by liquid scintillation counter (LS6500; Beckman Coulter, Fullerton, CA). In some experiments, GLUT1 and GLUT2 were ectopically expressed by using the pCAGGS expression vector [24] and glucose uptake was measured as described above.

2.5. Flow cytometry

To examine cell surface expression of GLUT1 and GLUT2, cells harvested in PBS containing 0.2% EDTA were incubated with rabbit polyclonal antibodies against GLUT1 or GLUT2 (1:200; Alpha Diagnostic International, San Antonio, TX, USA) on ice for 1 h. After being washed, the cells were incubated with FITC-labeled goat anti-rabbit IgG (1:200; BD Pharmingen, Franklin Lakes, NJ, USA) on ice for another 1 h. Analysis was carried out using flow cytometer and a total of 10,000 live cell events were measured. Results were displayed graphically as overlaying histograms demonstrating the shift of the mean FITC staining value.

Please cite this article in press as: Kasai D et al., HCV replication suppresses cellular glucose uptake through ..., J Hepatol (2009), doi:10.1016/j.jhep.2008.12.029

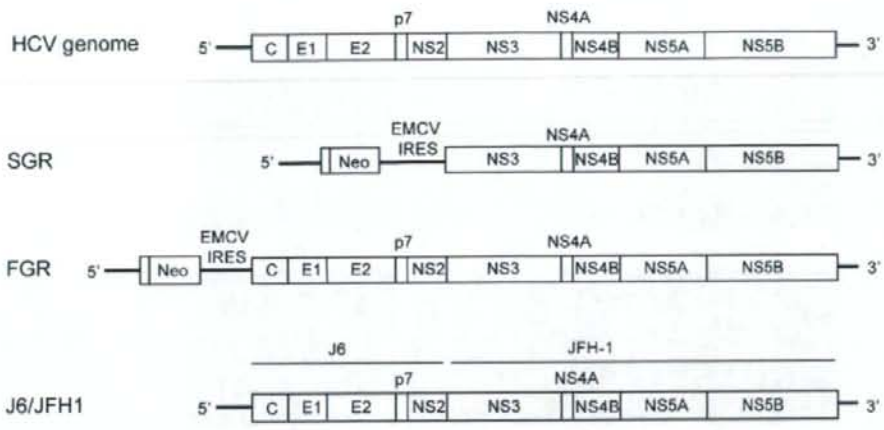

Fig. 1. The HCV genome and HCV RNA replicons. Schematic diagram of the HCV genome, SGR, FGR and the chimeric HCV J6/JFH1 genome are shown. EMCV IRES, encephalomyocarditis virus internal ribosome entry site; Neo, neomycin-resistance gene.

2.6. Real-time quantitative RT-PCR

Total cellular RNA was isolated using the TRIzol reagent (Invitrogen Corp., Carlsbad, CA, USA) and cDNA was generated using QuantiTect Reverse Transcription system (Qiagen, Valencia, CA, USA). Real-time quantitative PCR was performed on a SYBR *Premix Ex Taq* (Takara Bio, Kyoto, Japan) using SYBR green chemistry in ABI PRISM 7000 (Applied Biosystems, Foster, CA, USA). β-Glucuronidase was used as an internal control. The primers used are shown in Table 1.

2.7. Luciferase reporter assay

We constructed the human GLUT2 promoter-luciferase reporter gene (pGLUT2-1291Luc) by cloning a 1.6-kb genomic fragment that encompasses the human GLUT2 promoter (−1291 to +308) [14] into the pGL4 vector plasmid (Promega, Madison, WI, USA). pGLUT2-1291Luc thus contains a 1291-bp fragment of the human GLUT2 promoter upstream of the minimal promoter and the coding sequence of the *Photinus pyralis* (firefly) luciferase. pRL-CMV-*Renilla* (Promega) was used as an internal control. Cells were transfected with pGLUT2-1291Luc (1 μg) and pRL-CMV-*Renilla* (10 ng). After 24 h, a luciferase assay was performed by using Dual-luciferase reporter assay system (Promega). Firefly and *Renilla* luciferase activities were measured by Lumat LB 9501 (Berthold, Bad Wildbad, Germany). Firefly luciferase activity was normalized to *Renilla* luciferase activity for each sample.

2.8. Immunohistochemistry

Human adult liver autopsy materials and surgically removed liver tissues of patients with HCV- or HBV-associated hepatocellular carcinoma, and those with metastatic liver cancer were obtained with written informed consent. The tissues were fixed with 10% buffered formalin (pH 7.0), embedded in paraffin and sectioned at intervals of 4 μm. Immunohistochemical staining was performed with a DAKO ENVISION+ Kit (Dako, Glostrup, Denmark). In brief, fixed sections were treated with 3% hydrogen peroxide, and were autoclaved at 121 °C for 20 min. Then, the sections were incubated with a blocking solution and then with either anti-GLUT2 rabbit polyclonal antibody (Santa Cruz Biotechnology, Santa Cruz, CA, USA) or normal rabbit IgG (Santa Cruz Biotechnology) as a control. The sections were incubated with horseradish peroxidase-labeled polymer-conjugated goat anti-rabbit IgG, followed by incubation in a chromogenic solution. The sections were then counterstained with hematoxylin and examined with a light microscope. GLUT2 expression levels were arbitrarily determined by two examiners, including a pathologist, in a blinded manner.

2.9. Statistical analysis

Results were expressed as mean ± SEM. Statistical significance was evaluated by ANOVA, and statistical significance was defined as $P < 0.05$.

Table 1
Sequences and positions of the primers used in this study.

Gene name (GenBank ID)	Primer	Position	PCR product (bp)
GLUT2	5'-TGGGCTGAGGAAGAGACTGT-3'	279–298	461
(J03810)	5'-AGAGACTGAAGGATGGCTCG-3'	739–720	
GLUT1	5'-TGAACCTGCTGGCCTTC-3'	437–453	399
(AK292791)	5'-GCAGCTTCTTTAGCACA-3'	835–819	
HCV NS5B	5'-ACCAAGCTCAAACTCACTCCA-3'	9191–9211	119
(AJ238799)	5'-AGCGGGGTCGGGCACGAGACA-3'	9309–9289	
β-glucuronidase	5'-ATCAAAAACGCAGAAAATACG-3'	1747–1767	238
(M15182)	5'-ACGCAGGTGGTATCAGTCTTG-3'	1984–1964	

Please cite this article in press as: Kasai D et al., HCV replication suppresses cellular glucose uptake through ..., J Hepatol (2009), doi:10.1016/j.jhep.2008.12.029

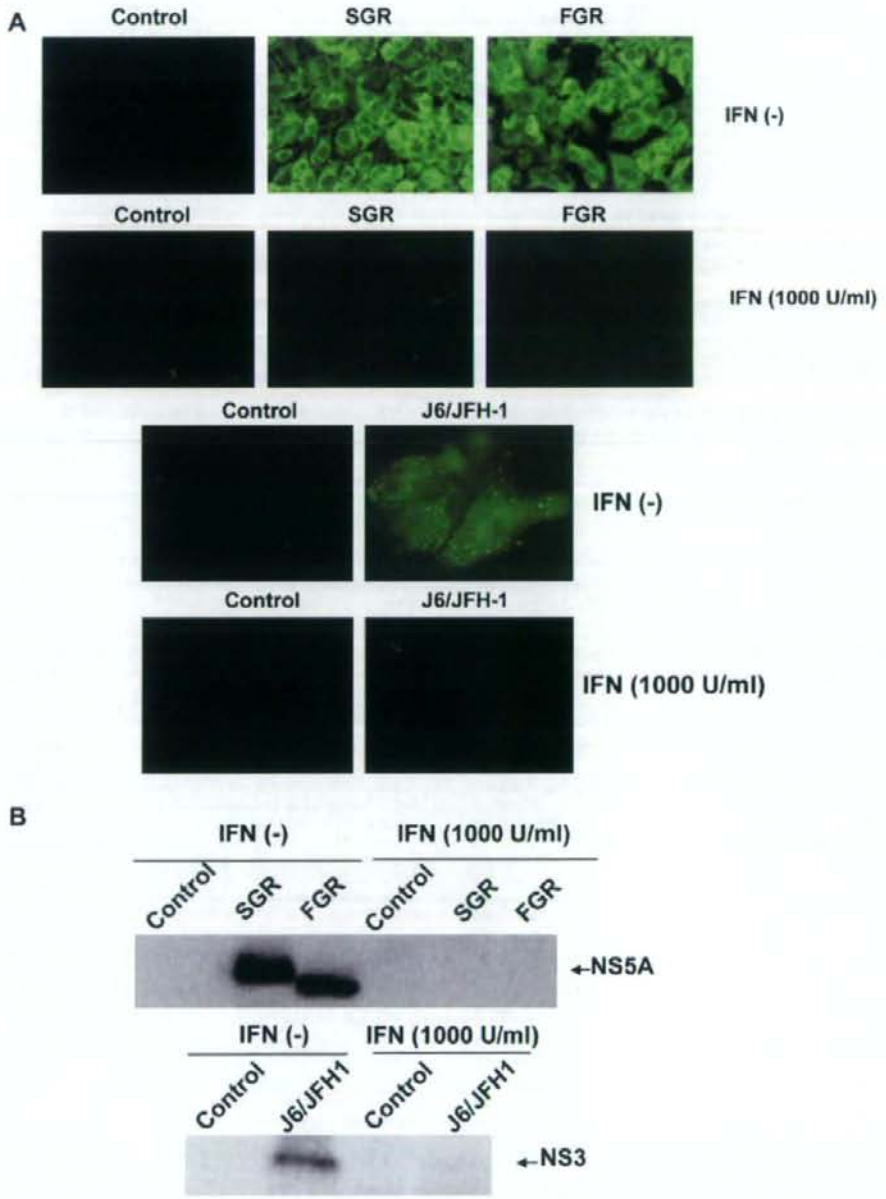

Fig. 2. Expression of HCV proteins in SGR, FGR, HCV-infected cells and the respective cells treated with IFN. (A) Cells were immunostained with anti-NS5A antibody (for SGR, FGR and the control cells) or anti-core antibody (for HCV-infected cells and the control). In parallel, cells were treated with IFN (1000 IU/ml) for 10 days to eliminate HCV replication before being subjected to immunostaining. (B) Cells were analyzed by immunoblotting with anti-NS5A antibody (upper panel) or anti-NS3 antibody (lower panel). In parallel, cells were treated with IFN (1,000 IU/ml) for 10 days to eliminate HCV replication before being subjected to immunoblotting.

Please cite this article in press as: Kasai D et al., HCV replication suppresses cellular glucose uptake through ..., J Hepatol (2009), doi:10.1016/j.jhep.2008.12.029

3. Results

3.1. HCV protein expression in SGR, FGR, HCV-infected cells and those treated with IFN

Immunofluorescence analysis revealed that almost all the cells in SGR and FGR cultures, and >90% of the cells in the HCV J6/JFH1-infected culture were positive for HCV antigens (Fig. 2A). Western blot analysis also confirmed HCV protein expression in SGR, FGR and HCV-infected cells (Fig. 2B). In some experiments, HCV replication in SGR, FGR and HCV-infected cells was eliminated by IFN treatment for 10 days (Fig. 2A and B).

3.2. Selective suppression of cellular glucose uptake by HCV replication

2-Deoxygluose uptake levels in SGR, FGR and HCV-infected cells were significantly suppressed by about 50–60%, compared with the control Huh-7.5 cells (Fig. 3A and B). On the other hand, thymidine uptake, which was used as a control, did not significantly differ among all the cells tested (data not shown). Moreover, glucose uptake levels in SGR, FGR and HCV-infected cells were restored by IFN treatment (Fig. 3A and B). These results strongly suggest that cellular glucose uptake is selectively suppressed by HCV RNA replication.

3.3. Down-regulation of cell surface expression of GLUT2 and GLUT1 by HCV replication

GLUT2 is the principal glucose transporter of hepatocytes *in vivo* while GLUT1 is expressed in a wide variety of cultured cells. We therefore examined cell surface expression of GLUT2 and GLUT1 by flow cytometry analysis. As shown in Fig. 4A, cell surface expression of GLUT2 and GLUT1 was markedly down-regulated in SGR and FGR cells, compared with the control. On the other hand, cell surface expression of transferrin receptor was not significantly suppressed in SGR or FGR, compared with the control, with the result ensuring the specificity of the down-regulation of GLUT2 and GLUT1 cell surface expression in SGR and FGR (Fig. 4A). Moreover, treatment of SGR and FGR cells with IFN restored the surface expression of GLUT2 and GLUT1 (Fig. 4A). These results suggest that HCV RNA replication specifically mediates down-regulation of GLUT2 and GLUT1.

Down-regulation of GLUT2 surface expression was observed also in HCV-infected cells (Fig. 4B). On the other hand, down-regulation of GLUT1 surface expression was only marginal and, compared to that of GLUT2, less evidently observed in HCV-infected cells. As a control, cell surface expression of transferrin receptor did not differ at all between HCV-infected cells and the control. Again, treatment of HCV-infected cells with IFN restored surface expression of GLUT2 (Fig. 4B).

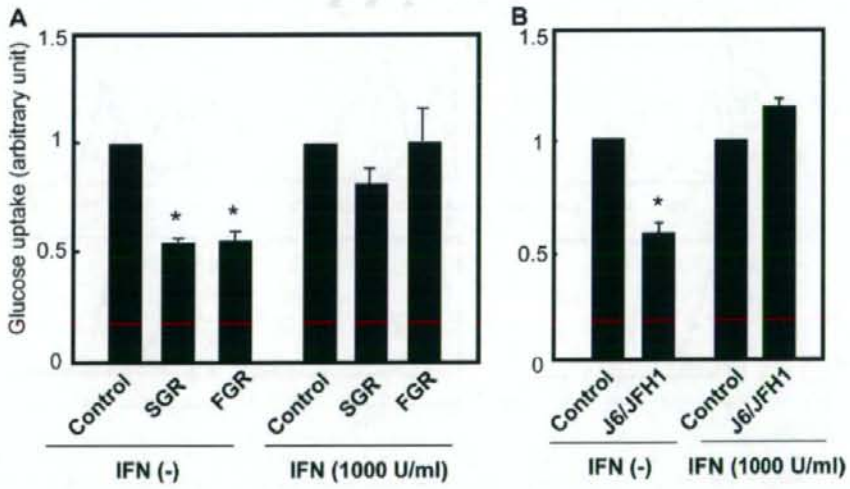

Fig. 3. Selective suppression of cellular glucose uptake by HCV replication. (A) Uptake of 2-deoxy-D-[1,2-^{3}H] glucose in SGR, FGR and HCV-negative control. In parallel, cells were treated with IFN (1000 IU/ml) for 10 days to eliminate HCV replication before being subjected to glucose uptake analysis. Data represent mean ± SEM of four independent experiments and the values for the control cells were arbitrarily expressed as 1.0. $^*P < 0.01$, compared with the control. (B) Uptake of 2-deoxy-D-[1,2-^{3}H] glucose in J6/JFH-1-infected cells and the uninfected control. In parallel, cells at 5 days after infection were treated with IFN (1000 IU/ml) for 10 days to eliminate HCV replication before being subjected to glucose uptake analysis.

Please cite this article in press as: Kasai D et al., HCV replication suppresses cellular glucose uptake through ..., J Hepatol (2009), doi:10.1016/j.jhep.2008.12.029

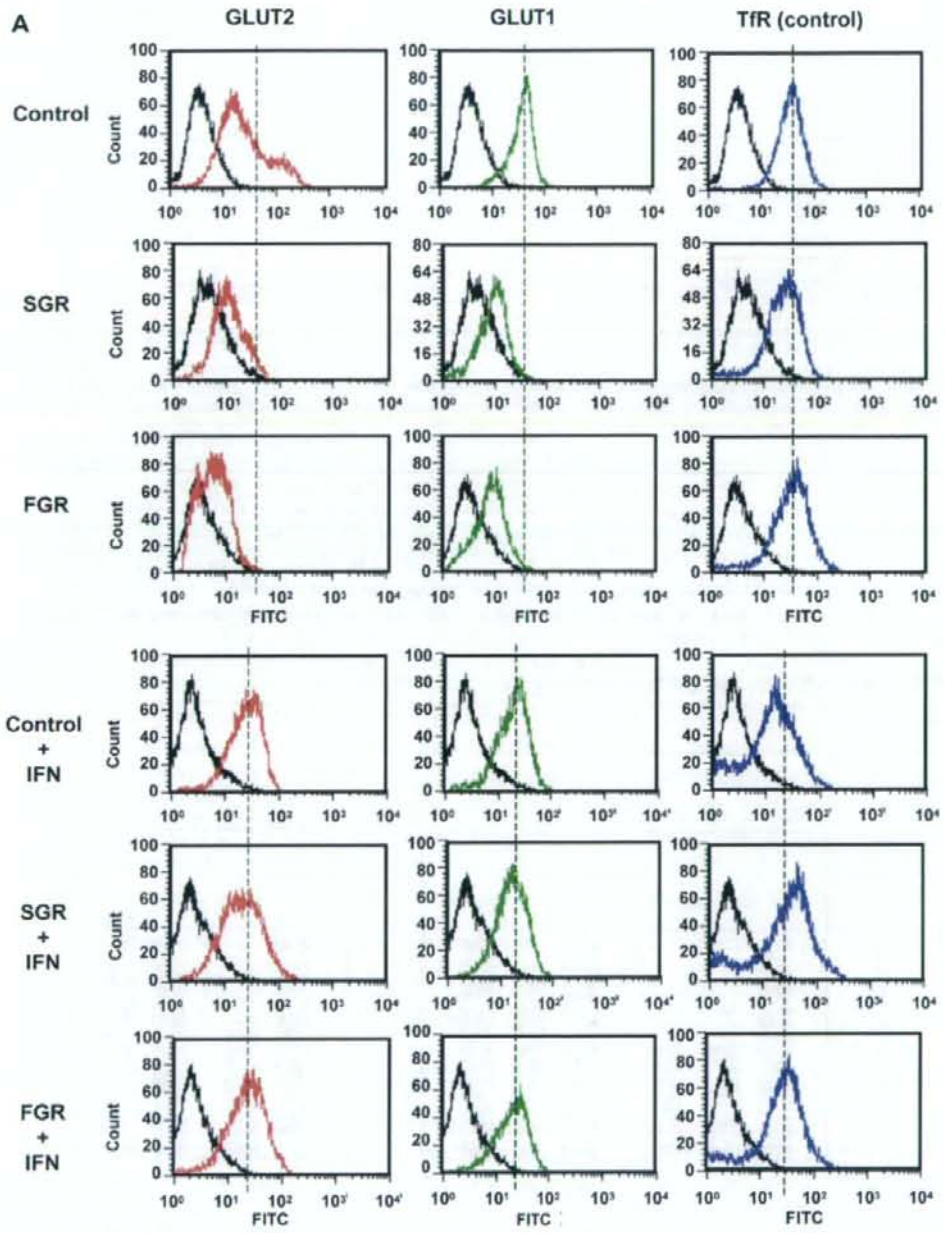

Fig. 4. Down-regulation of cell surface expressions of GLUT2 and GLUT1 by HCV replication. (A) SGR, FGR, the HCV-negative control cells were stained with specific antibodies, followed by FITC-conjugated second antibody (GLUT2, red line; GLUT1, green line) or stained with FITC-conjugated antibody alone (black line). Transferrin receptor (TfR) served as a control (blue line). In parallel, cells were treated with IFN (1000 IU/ml) for 10 days to eliminate HCV replication before being subjected to flow cytometry. (B) HCV-infected cells and the uninfected control were analyzed by flow cytometry as in (A). In parallel, cells at 5 days after infection were treated with IFN (1000 IU/ml) for 10 days to eliminate HCV replication before being subjected to flow cytometry analysis.

Please cite this article in press as: Kasai D et al., HCV replication suppresses cellular glucose uptake through ..., J Hepatol (2009), doi:10.1016/j.jhep.2008.12.029